Molecular Cell
Article

Caenorhabditis elegans drp-1 and *fis-2* Regulate Distinct Cell-Death Execution Pathways Downstream of *ced-3* and Independent of *ced-9*

David G. Breckenridge,[1] Byung-Ho Kang,[1,2] David Kokel,[1] Shohei Mitani,[3] L. Andrew Staehelin,[1] and Ding Xue[1,*]
[1]Department of Molecular, Cellular and Developmental Biology, University of Colorado, Boulder, CO 80309, USA
[2]Department of Microbiology and Cell Science, Integrated Center for Biotechnology Research, University of Florida, Gainesville, FL 32608, USA
[3]Department of Physiology, Tokyo Women's Medical University, School of Medicine, and CREST, JST, Tokyo, 162-8666, Japan
*Correspondence: ding.xue@colorado.edu
DOI 10.1016/j.molcel.2008.07.015

SUMMARY

The dynamin family of GTPases regulate mitochondrial fission and fusion processes and have been implicated in controlling the release of caspase activators from mitochondria during apoptosis. Here we report that profusion genes *fzo-1* and *eat-3* or the profission gene *drp-1* are not required for apoptosis activation in *C. elegans*. However, minor proapoptotic roles for *drp-1* and *fis-2*, a homolog of human Fis1, are revealed in sensitized genetic backgrounds. *drp-1* and *fis-2* function independent of one another and the Bcl-2 homolog CED-9 and downstream of the CED-3 caspase to promote elimination of mitochondria in dying cells, an event that could facilitate cell-death execution. Interestingly, CED-3 can cleave DRP-1, which appears to be important for DRP-1's proapoptotic function, but not its mitochondria fission function. Our findings demonstrate that mitochondria dynamics do not regulate apoptosis activation in *C. elegans* and reveal distinct roles for *drp-1* and *fis-2* as mediators of cell-death execution downstream of caspase activation.

INTRODUCTION

Genetic studies in *C. elegans* have led to the identification of a central killing pathway that is conserved between nematodes and humans (Horvitz, 1999). In cells destined to undergo apoptosis, the BH3-only proapoptotic protein EGL-1 is upregulated and binds to CED-9, an antiapoptotic Bcl-2 homolog, resulting in the disassociation of CED-4, a mammalian Apaf-1 homolog, from the CED-4/CED-9 complex tethered on the surface of mitochondria (Horvitz, 1999). CED-4 subsequently oligomerizes and activates the CED-3 caspase zymogen (Yan et al., 2006), which then orchestrates numerous cell disassembly and cleanup processes, including fragmentation of chromosomal DNA (Parrish et al., 2001; Wang et al., 2002) and removal of cell corpses (Reddien and Horvitz, 2004).

The cell-death activation process in mammals appears to be far more complex and involves release of proapoptotic factors from the intermembrane space of mitochondria. For example, Bcl-2 family proteins impinge on the structure of mitochondria, causing dramatic changes in mitochondria size and cristae structure and ultimately increased permeability of the outer mitochondrial membrane to caspase activators such as cytochrome c and Smac/Diablo (Antignani and Youle, 2006; Cereghetti and Scorrano, 2006). In addition, dynamin family GTPases, such as DRP1, which is required for mitochondrial fission, and OPA1 and MFN1/FZO1, which control inner and outer mitochondrial membrane fusion events, respectively, have been reported to mediate some of the structural rearrangements of mitochondria observed during apoptosis (Cereghetti and Scorrano, 2006; Chan, 2006). Downregulation of MFN1/FZO1 and concurrent activation of DRP1 was shown to cause dramatic fragmentation of the mitochondrial network during apoptosis (Frank et al., 2001; Karbowski et al., 2002, 2004), whereas disruption of OPA1 oligomers leads to remodeling of inner membrane cristae (Cipolat et al., 2006; Frezza et al., 2006). These changes in mitochondrial network and structure, in some cellular contexts (Frank et al., 2001; Frezza et al., 2006; Lee et al., 2004), but not in others (Delivani et al., 2006; Estaquier and Arnoult, 2007; Parone et al., 2006), appear to affect the release of cytochrome c from the mitochondrial intermembrane space and subsequent caspase activation. Fis1, which may recruit DRP1 to the outer mitochondrial membrane (Okamoto and Shaw, 2005), has also been suggested to mediate mitochondrial fission and apoptosis signaling in yeast (Fannjiang et al., 2004; Mozdy et al., 2000) and in mammals (Alirol et al., 2006; James et al., 2003; Lee et al., 2004; Parone et al., 2006). Recently, *C. elegans drp-1* was reported to promote *ced-9*-dependent mitochondrial fission and apoptosis, possibly by releasing caspase activating factors from mitochondria (Jagasia et al., 2005), leading to the hypothesis that apoptotic mitochondrial fission is an evolutionarily conserved aspect of caspase activation. However, this hypothesis has yet to be substantiated by genetic analysis. As a result, the exact roles of mitochondrial fission and fusion processes in apoptosis and their positions in the cell-death pathway with respect to caspase activation and Bcl-2 family proteins remain unclear (Parone and Martinou, 2006).

Here, we report systematic genetic and cell biological characterization of the contribution of mitochondrial fission and fusion processes to programmed cell death in *C. elegans.* Surprisingly, we found that loss of the mitochondrial dynamin genes, *drp-1*,

fzo-1, and *eat-3* (an OPA1 homolog), does not affect the activation or the kinetics of programmed cell death in *C. elegans*, even though loss of *drp-1* blocks mitochondrial fission and loss of *fzo-1* or *eat-3* prevents mitochondrial fusion and causes excessive mitochondrial fission. However, minor and independent roles for *drp-1* and *fis-2* (a Fis1 homolog) downstream of CED-3 activation in promoting mitochondrial elimination and cell-death execution were uncovered in sensitized genetic backgrounds. Furthermore, we find that DRP-1 can be cleaved by CED-3 in vitro, and such cleavage appears to be important for DRP-1's pro-apoptotic function in vivo, but not its mitochondrial fission function, suggesting that the proapoptotic function of DRP-1 can be separated from its mitochondrial fission function. Our results argue against a conserved, caspase-activating role for mitochondrial dynamins and highlight distinct roles for *drp-1* and *fis-2* downstream of caspase activation.

RESULTS

drp-1, *fzo-1*, and *eat-3* Regulate Mitochondrial Fission and Fusion in *C. elegans*

The *C. elegans* genome contains three genes, *fzo-1*, *eat-3*, and *drp-1*, which encode orthologs of MFN1/FZO1, OPA1, and DRP1, respectively. Two homologs of Fis1, *fis-1* and *fis-2*, exist in the worm, and they share a similar degree of sequence homology to the human and yeast Fis1 proteins (Figure S1 available online). For each of these genes, we obtained deletion allele(s) that disrupt the respective coding sequences and are expected to be strong loss-of-function (*lf*) or null mutations (Figure S2).

fzo-1(tm1133), *eat-3(ad426)*, and *eat-3(tm1107)* animals exhibit slow growth, reduced brood sizes, and high percentages of embryonic lethality (Avery, 1993), probably due to compromised mitochondrial functions important for the vitality of the cells (Chan, 2006). The *eat-3(ad426)* mutation causes a Val 328 to Ile substitution within the GTPase domain (Avery, 1993; D.G.B. and D.X., unpublished data). *drp-1(tm1108)* animals also exhibit reduced brood sizes and a high percentage of embryonic lethality, whereas *fis-1(tm1867)*, *fis-1(tm2227)*, *fis-2(gk363)*, and *fis-2(tm1832)* animals, as well as *fis-1(tm1867); fis-2(gk363)* double mutant animals, appear superficially wild-type (data not shown). Staining of live embryos with tetramethyl rhodamine ester (TMRE), a mitochondria-specific dye, and thin section electron microcopy analysis revealed striking differences in the overall connectivity of the mitochondrial network in embryos of the various mutant backgrounds (Figures 1A–1N). Compared to wild-type *N2* animals, TMRE-stained mitochondria in *drp-1(tm1108)* embryos appeared clumpy and highly fused (Figures 1A and 1B), and the number of mitochondria observed in EM sections of *drp-1(tm1108)* embryos was low. But individual mitochondria were often very long, with an increased longitudinal mean length of 2.28 μm, compared with 0.95 μm mean length in *N2* animals (Figures 1I, 1J, and 1N). These results suggest a reduction in mitochondrial fission in *drp-1(tm1108)* animals (Labrousse et al., 1999). Conversely, mitochondria appeared highly fragmented in *fzo-1(tm1133)*, *eat-3(ad426)*, and *eat-3(tm1107)* embryos (Figures 1F and 1G and data not shown). Electron micrographs of *fzo-1(tm1133)* and *eat-3(ad426)* embryos displayed an increased number of spherical mitochondria with rather uniform length (mean lengths of 0.38 μm and 0.44 μm, respectively) (Figures 1L and 1M). Therefore, *fzo-1* and *eat-3* appear to be required for mitochondrial fusion in *C. elegans*. In addition, mitochondria in *eat-3(ad426)* embryos had disrupted cristae structures (Figure S3), suggesting that, like OPA1 in mammals, EAT-3 is required for maintenance of mitochondrial cristae (Frezza et al., 2006). Mitochondria in the *fzo-1(tm1133); drp-1(tm1108)* double mutant were highly connected and indistinguishable from those in *drp-1(tm1108)* single mutant embryos (compare Figures 1B and 1H), indicating that *drp-1* is required for the mitochondrial fragmentation observed in *fzo-1* mutants (Bleazard et al., 1999). Similar mitochondrial morphologies were observed in body wall muscle cells, the germline, and the intestinal cells of each mutant strain (data not shown). The defects in mitochondrial morphology observed in *drp-1(tm1108)*, *fzo-1(tm1133)*, and *eat-3(ad426)* animals are similar to those described for loss-of-function mutants of their respective homologs in yeast, mouse, and humans (Chan, 2006). Mitochondrial connectivity appears normal in *fis-1(tm1867)*, *fis-1(tm2227)*, *fis-2(gk363)*, and *fis-2(tm1832)* single mutants and in the *fis-1(tm1867); fis-2(gk363)* double mutant (Figures 1C, 1D, 1E, and 1K and data not shown), suggesting that, unlike in yeast and mammals (Okamoto and Shaw, 2005; Chan, 2006), *C. elegans fis* genes are not required for mitochondrial fission. However, it is possible that *fis-1* and *fis-2* function redundantly with other unknown genes to regulate mitochondrial fission.

Cell Death Occurs Normally in the Absence of Mitochondrial Fission or Fusion in *C. elegans*

We next examined the kinetics of programmed cell death in various mitochondrial fission and fusion mutants by conducting a time course analysis of cell-corpse appearance during embryo development. In this assay, mutants strongly defective in cell death have few cell corpses at all stages of embryonic development (Ellis and Horvitz, 1986; Stanfield and Horvitz, 2000), mutants that are weakly defective in cell death often display a delay in cell-corpse appearance or reduced cell-corpse numbers (Parrish et al., 2001; Stanfield and Horvitz, 2000; Wang et al., 2002), and mutants defective in antiapoptotic genes or genes involved in cell-corpse engulfment have increased cell-corpse numbers at all embryonic stages (Hedgecock et al., 1983; Ellis et al., 1991; Hengartner et al., 1992; Bloss et al., 2003). Although *fzo-1(tm1133)*, *eat-3(ad426)*, and *eat-3(tm1107)* animals had highly fragmented mitochondria (Figure 1), the numbers of cell corpses in these mutants were normal at all stages of embryonic development (Figure S4A), indicating that excessive mitochondrial fragmentation per se does not cause ectopic cell deaths in *C. elegans*. We confirmed this finding in a sensitized genetic background, *ced-1(e1735)*, where engulfment of apoptotic cells is blocked and a small increase in cell deaths will result in a greater increase in the number of persistent cell corpses (Hedgecock et al., 1983; Ellis et al., 1991; Bloss et al., 2003) (Figure S4B). The cell-corpse numbers or the kinetics of cell-corpse appearance were also unaffected in *drp-1(tm1108)* animals (Figure S4C), even though mitochondria were constitutively fused (Figure 1). *fis-1(tm1867)*, *fis-2(gk363)*, and *fis-2(tm1832)* single mutants, and *fis-1(tm1867); fis-2(gk363)* double mutant animals also had cell-corpse profiles that did not significantly

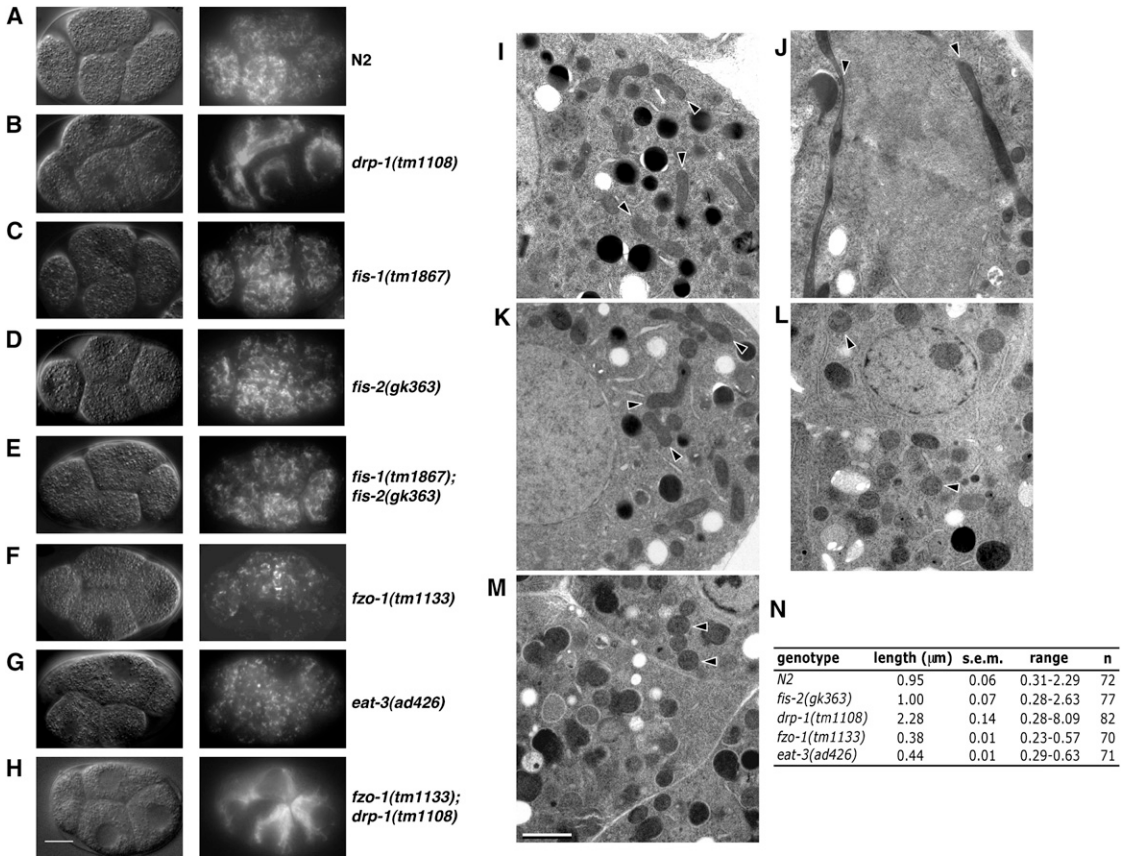

genotype	length (μm)	s.e.m.	range	n
N2	0.95	0.06	0.31-2.29	72
fis-2(gk363)	1.00	0.07	0.28-2.63	77
drp-1(tm1108)	2.28	0.14	0.28-8.09	82
fzo-1(tm1133)	0.38	0.01	0.23-0.57	70
eat-3(ad426)	0.44	0.01	0.29-0.63	71

Figure 1. Mitochondrial Morphology in Mitochondrial Fission and Fusion Mutant Embryos

(A–H) Live imaging of mitochondrial morphology. The indicated strains were stained with TMRE, and four-cell stage embryos were visualized by Differential Interference Contrast (DIC, left) and rhodamine fluorescence (right) microscopy. Compared with the wild-type embryo (A), the mitochondrial network is highly connected in the *drp-1(tm1108)* and *fzo-1(tm1133); drp-1(tm1108)* embryos (B and H), indistinguishable from that of the wild-type embryo in *fis-1(tm1867)*, *fis-2(gk363)*, and *fis-1(tm1867); fis-2(gk363)* embryos (C–E), and highly fragmented in *fzo-1(tm1133)* and *eat-3(ad426)* embryos (F and G). Scale bar represents 10 μm. (I–M) Representative electron micrographs of embryos from the following strains are shown: *N2* (I), *drp-1(tm1108)* (J), *fis-2(gk363)* (K), *fzo-1(tm1133)* (L), and *eat-3(ad426)* (M). Scale bar represents 1 μM. Arrows indicate the longitudinal axis of mitochondria. (N) Quantification of the mean mitochondrial length. Randomly selected mitochondria from electron micrographs were measured along their longitudinal axis. For each strain, mitochondria were selected from over 10 different embryos inside at least two thin-sectioned gravid adult animals. SEM, standard error of the mean. n, the number of mitochondria scored.

differ from that of wild-type animals (Figure S4C). Altogether, these results suggest that defects in mitochondria fusion or fission do not obviously affect programmed cell death in *C. elegans*.

We also examined whether any of these mutations can block cell death by counting the number of inappropriately surviving cells that normally die during the development of the anterior pharynx (Ellis and Horvitz, 1986; Wang et al., 2002). No extra surviving cells were found in the anterior pharynx of any of the individual mitochondrial fission or fusion mutants or in the *fis-1(tm1867); fis-2(gk363)* double mutant (Table 1). Thus, programmed cell death occurs normally in *C. elegans* in the absence of either mitochondrial fusion or fission.

drp-1 and *fis-2* Have Minor, Independent Roles during Programmed Cell Death

Our analysis of the *drp-1(tm1108)* mutant, which has no detectable DRP-1 protein expression (Figure S5) and thus represents a strong loss-of-function or null mutant, contrasts with the conclusion of a previous report that *drp-1* plays a significant role in promoting apoptosis in *C. elegans* (Jagasia et al., 2005). The conclusion by Jagasia et al. was based on the observation that ectopic expression of a dominant-negative DRP-1(K40A) mutant resulted in the survival of 2 to 3 extra cells in the anterior pharynx of transgenic animals. The different cell-death phenotypes observed between *drp-1(tm1108)* animals and animals overexpressing *drp-1*(K40A) may reflect an off-target effect of the dominant-negative mutant, since overexpresssion of DRP-1(K40A) induced a similar number of extra cells in *drp-1(tm1108)* animals (without endogenous DRP-1) as in wild-type animals (Table S1). This result indicates that the endogenous DRP-1 protein is not a target of DRP-1(K40A).

Since some weak cell-death mutations that do not block cell death on their own can enhance the cell-death defect caused by weak alleles of *ced-3* or *ced-4* (Parrish et al., 2001; Stanfield and Horvitz, 2000; Wang et al., 2002), we constructed strains

Table 1. Loss of Individual Mitochondrial Fission or Fusion Genes Does Not Cause Inappropriate Survival of Cells that Normally Die in the Anterior Pharynx

Genotype	Number of Extra Cells			
	Mean	SEM	Range	n
N2	0.1	0.1	0–1	40
eat-3(ad426)	0.1	0.1	0–1	32
eat-3(tm1107)	0.1	0.1	0–1	35
fzo-1(tm1133)	0.1	0.1	0–1	30
fis-1(tm1867)	0.1	0.1	0–1	30
fis-1(tm2227)	0.1	0.1	0–1	30
fis-2(gk363)	0.1	0.1	0–1	20
fis-2(tm1832)	0.2	0.1	0–1	30
fis-1(tm1867); fis-2(gk363)	0.1	0.1	0–1	20
drp-1(tm1108)	0.1	0.1	0–1	27
drp-1(tm1108); fis-2(gk363)[a]	0.6	0.2	0–2	23
drp-1(tm1108); fis-2(tm1832)[b]	0.5	0.1	0–2	31

The number of extra cells in the anterior pharynx of the indicated animals was counted as described in the Experimental Procedures. SEM, standard error of the mean. Unpaired two-tailed t test, compared with N2 animals: [a]p = 0.0017, [b]p = 0.0011. Others have p values > 0.05.

Table 2. *drp-1* and *fis-2* Have Minor, Independent Roles during Programmed Cell Death

Genotype	Number of Extra Cells			
	Mean	SEM	Range	n
ced-3(n2438)	1.3	0.2	0–4	40
eat-3(ad426); ced-3(n2438)	1.6	0.2	0–4	33
fzo-1(tm1133); ced-3(n2438)	1.5	0.3	0–5	20
drp-1(tm1108) ced-3(n2438)[a]	2.5	0.3	0–4	32
fis-1(tm1867); ced-3(n2438)	1.1	0.3	0–3	20
fis-1(tm2227); ced-3(n2438)	1.5	0.2	0–4	44
ced-3(n2438); fis-2(gk363)[b]	2.8	0.2	1–7	38
ced-3(n2438); fis-2(tm1832)[c]	2.5	0.2	1–4	26
fis-1(tm1867); drp-1(tm1108) ced-3(n2438)	2.4	0.3	0–4	20
fis-1(tm1867); ced-3(n2438); fis-2(gk363)[d]	2.6	0.4	1–6	20
drp-1(tm1108) ced-3(n2438); fis-2(gk363)[e]	3.9	0.2	2–6	20
drp-1(tm1108) ced-3(n2438); fis-2(tm1832)[f]	3.7	0.3	1–7	34
ced-4(2273)	1.6	0.3	0–4	25
ced-4(n2273); fis-2(gk363)[g]	2.9	0.2	1–4	25
ced-4(n2273) drp-1(tm1108)[h]	2.7	0.3	1–6	24
ced-4(n2273); drp-1(tm1108); fis-2(gk363)[i]	4.3	0.2	3–7	24
ced-3(n2438); control(RNAi)	1.5	0.1	0–4	50
ced-3(n2438); wah-1(RNAi)[j]	2.4	0.1	0–4	43
ced-3(n2438); cps-6(RNAi)[k]	2.4	0.2	0–5	44
drp-1(tm1108) ced-3(n2438); control(RNAi)	2.2	0.3	0–4	24
drp-1(tm1108) ced-3(n2438); wah-1(RNAi)[l]	3.9	0.2	1–6	45
drp-1(tm1108) ced-3(n2438); cps-6(RNAi)[m]	4.4	0.4	1–7	27
ced-3(n2438); fis-2(gk363); control(RNAi)	2.2	0.2	0–5	28
ced-3(n2438); fis-2(gk363); wah-1(RNAi)[n]	3.5	0.1	1–5	46
ced-3(n2438); fis-2(gk363); cps-6(RNAi)[o]	3.9	0.2	2–6	34
drp-1(tm1108) ced-3(n2438); fis-2(gk363); control(RNAi)	3.6	0.2	1–6	29
drp-1(tm1108) ced-3(n2438); fis-2(gk363); wah-1(RNAi)[p]	5.3	0.3	3–8	36
drp-1(tm1108) ced-3(n2438); fis-2(gk363); cps-6(RNAi)[q]	5.0	0.3	2–8	29

The number of extra cells in the anterior pharynx of the indicated animals was counted. All data involving the *ced-3(n2438)* strains were confirmed by multiple independent blind test analyses. SEM, standard error of the mean. Unpaired two-tailed t test, compared with *ced-3(n2438)* animals: [a]p = 0.0012, [b]p = 3.4×10^{-5}, [c]p = 6.3×10^{-5}, [d]p = 0.0018, [e]p = 2.1×10^{-11}, and [f]p = 2.7×10^{-9}; compared with *ced-4(n2273)* animals: [g]p = 0.006, [h]p = 0.043, and [i]p = 3.0×10^{-9}; compared with *control*(RNAi) treatment of the same strain: [j]p = 8.8×10^{-5}, [k]p = 2.8×10^{-5}, [l]p = 1.3×10^{-5}, [m]p = 9.0×10^{-8}, [n]p = 6.3×10^{-6}, [o]p = 2.7×10^{-7}, [p]p = 8.7×10^{-6}, and [q]p = 1.1×10^{-4}. Others have p values > 0.05.

carrying each of the mitochondrial fission or fusion mutant alleles in a weak *ced-3* loss-of-function background (*n2438*) to determine if *fzo-1*, *eat-3*, *drp-1*, *fis-1*, or *fis-2* might play a facilitatory role in programmed cell death. Analysis of *fzo-1(tm1133); ced-3(n2438)* animals and *eat-3(ad426); ced-3(n2438)* animals did not reveal a significant decrease or increase in the number of extra cells compared with *ced-3(n2438)* animals (Table 2), confirming that *eat-3* and *fzo-1* do not affect cell death in *C. elegans*. However, analysis of *drp-1(tm1108) ced-3(n2438)* animals revealed a small but significant increase in the number of extra cells over that observed in *ced-3(n2438)* animals; 2.5 extra cells were seen in the anterior pharynx of *drp-1(tm1108) ced-3(n2438)* animals compared to 1.3 extra cells seen in *ced-3(n2438)* animals ($p < 0.005$, unpaired two-tailed t test). A similar increase in extra cells was observed in *ced-3(n2438); fis-2(gk363)*, *ced-3(n2438); fis-2(tm1832)*, and *fis-1(tm1867); ced-3(n2438); fis-2(gk363)* animals, but not in *fis-1(tm1867); ced-3(n2438)* or *fis-1(tm2227); ced-3(n2438)* animals, suggesting that *fis-2*, but not *fis-1*, also affects apoptosis in the worm. The different effects of *fis-1* and *fis-2* on somatic apoptosis may be due to the fact that *fis-1* expression is enriched in the germline, whereas *fis-2* expression is enriched in the soma (Reinke et al., 2004). However, we have not detected a germ cell-death defect in *fis-1(tm1867)* animals, even in sensitized genetic backgrounds (data not shown).

drp-1(tm1108) or *fis-2(gk363)* also weakly increased the number of extra cells observed in a weak *ced-4(n2273)* mutant background (Table 2), suggesting that *drp-1* and *fis-2* alleles can enhance the cell-death defect in different genetic backgrounds. Thus, *drp-1* and *fis-2* play minor roles in cell death, which are only observable in sensitized genetic backgrounds. Importantly, a GFP::FIS-2 fusion protein localizes to mitochondria (Figure S6), suggesting that FIS-2, like DRP-1 (Labrousse et al., 1999), exerts its proapoptotic function at this organelle.

Given that in yeast and mammals, DRP1 and FIS1 proteins can interact and promote mitochondrial fission (Okamoto and Shaw, 2005; Yu et al., 2005), it would seem likely that *drp-1* and *fis-2* function in the same cell-death pathway in *C. elegans*. If so, animals doubly mutant for *drp-1* and *fis-2* would have the same cell-death defect as either of the single mutants. Alternatively,

if these two genes function in different cell-death pathways, a more severe cell-death defect would be observed in the *drp-1; fis-2* double mutant. As shown in Figure S4C, *drp-1(tm1108); fis-2(gk363)* and *drp-1(tm1108); fis-2(tm1832)* double mutants had significantly fewer cell corpses than N2 and the single mutant animals, suggesting a reduction in cell death. Moreover, half of the *drp-1(tm1108); fis-2(gk363)* and *drp-1(tm1108); fis-2(tm1832)* animals had at least one and sometimes two extra cells in their anterior pharynx (a mean of 0.6 and 0.5 extra cell, respectively), which were only occasionally seen in N2 and the single mutant animals (Table 1), suggesting that some cells fail to undergo programmed cell death in these double mutants. Furthermore, *drp-1(tm1108)* and *fis-2(lf)* mutations additively enhanced the defect of the *ced-3(n2438)* mutant, resulting in an average of 3.7–3.9 extra cells in *drp-1(tm1108) ced-3(n2438); fis-2(lf)* animals, compared to 2.5–2.8 extra cells seen in *drp-1(tm1108) ced-3(n2438)* or *ced-3(n2438); fis-2(lf)* animals (Table 2, $p < 0.005$). *drp-1(tm1108)* and *fis-2(gk363)* mutations also additively enhanced the cell-death defect of the *ced-4(n2273)* mutant (Table 2). Given that *drp-1(tm1108)* and *fis-2(tm1832)* mutations are putative null alleles (Figures S2, S5, and S7) and can additively reduce cell death, *drp-1* and *fis-2* likely function independent of each other during apoptosis. However, the possibility that they have partially redundant functions cannot be ruled out. Consistent with the proposal that *drp-1* and *fis-2* function independently during apoptosis, overexpression of FIS-2 could induce ectopic apoptosis in *C. elegans* independent of *drp-1* (Table S2), whereas overexpression of a FIS-2(1-124) mutant lacking its transmembrane domain did not. On the other hand, overexpression of *drp-1* did not induce ectopic apoptosis (Table S2); however, overexpression of *drp-1* did cause excessive mitochondrial fission shortly after overexpression (data not shown) and could rescue the apoptosis and mitochondrial fission defects observed in *drp-1(tm1108) ced-3(n2438)* animals (Figure S8).

drp-1 and *fis-2* Act Independently of *ced-9* during Programmed Cell Death

BAX, a mammalian proapoptotic Bcl-2 family member, was reported to promote mitochondria fission and colocalize with DRP1 at sites of mitochondrial fission during apoptosis (Frank et al., 2001; Karbowski et al., 2002), leading to the hypothesis that these two proteins function together to cause apoptotic mitochondrial fission (Youle and Karbowski, 2005). In *C. elegans*, Jagasia et al. reported that the Bcl-2 homolog *ced-9* is required for *drp-1*-mediated mitochondrial fission and proposed that CED-9, like BAX, functions with DRP-1 to promote mitochondrial fragmentation and apoptosis by releasing caspase activating factors from mitochondria (Jagasia et al., 2005). A proapoptotic function for *ced-9* was first suggested by the finding that in weak *ced-3(lf)* mutants, *ced-9(lf)* mutations unexpectedly increase, rather than decrease (as expected of its antiapoptotic function), the number of extra surviving cells in the anterior pharynx (Hengartner and Horvitz, 1994). This finding was interpreted as evidence that *ced-9* has both proapoptotic and antiapoptotic functions. If *drp-1* or *fis-2* acts in the *ced-9* proapoptotic pathway, then *drp-1(tm1108)* and *fis-2(gk363)* alleles are not expected to increase the number of extra cells in the *ced-9(n2812); ced-3(n2438)* mutant, which contains a putative *ced-9* null allele (Hengartner et al., 1992). As shown in Table 3, *ced-9(n2812); ced-3(n2438)* animals have an average of 7.2 extra cells in the anterior pharynx compared to 1.3 extra cells observed in *ced-3(n2438)* animals. *ced-9(n2812); drp-1(tm1108) ced-3(n2438)* animals had an average of 8.4 extra cells, displaying a small but significant increase in extra cells over *ced-9(n2812); ced-3(n2438)* animals ($p = 0.008$, unpaired two-tailed t test). In *ced-9(n2812); ced-3(n2438); fis-2(gk363)* animals, the number of extra cells was raised to 8.6, again significantly higher than that of the *ced-9(n2812); ced-3(n2438)* animals ($p = 0.0003$, unpaired two-tailed t test). Moreover, *ced-9(n2812); drp-1(tm1108) ced-3(2438); fis-2(gk363)* animals showed a further increase in extra cells to an average of 9.8 (Table 3). The fact that *drp-1(tm1108)* and *fis-2(gk363)* null alleles additively increase the number of extra cells observed in the absence of *ced-9* activity strongly suggests that DRP-1 and FIS-2 function independently of CED-9 to promote programmed cell death in *C. elegans*.

Table 3. *drp-1* and *fis-2* Function Independently of *ced-9* during Programmed Cell Death

Genotype	Number of Extra Cells			
	Mean	SEM	Range	n
ced-3(n2438)	1.3	0.2	0–4	20
ced-9(n2812); ced-3(n2438)	7.2	0.3	5–10	23
ced-9(n2812); drp-1(tm1108) ced-3(n2438)[a]	8.4	0.3	5–11	20
ced-9(n2812); ced-3(n2438); fis-2(gk363)[b]	8.6	0.2	6–10	20
ced-9(n2812); ced-3(n2438) drp-1(tm1108); fis-2(gk363)[c]	9.8	0.4	7–13	21

The number of extra cells in the anterior pharynx of the indicated animals was counted as described in Table 1. All strains carried the *dpy-4(e1166)* allele. All data were confirmed by multiple independent blind test analyses. SEM, standard error of the mean. Unpaired two-tailed t test, compared with *ced-9(n2812); ced-3(n2438)* animals: [a]$p = 0.0084$, [b]$p = 3.3 \times 10^{-4}$, and [c]$p = 2.3 \times 10^{-6}$.

drp-1 and *fis-2* Act Downstream of, or in Parallel to, *ced-3* to Promote Cell Death

We conducted further genetic epistasis analysis to determine where *drp-1* and *fis-2* act in the programmed cell-death pathway in relation to *egl-1* and *ced-3*. Ectopic expression of *egl-1* driven by the *C. elegans* heat shock promoters (P_{hsp}*egl-1*) resulted in increased apoptosis in *C. elegans* embryos and the accumulation of over 40 cell corpses (Table 4). EGL-1-induced cell killing was completely blocked by a strong loss-of-function *ced-3* mutation (*n717*) but was not affected by either the *drp-1(tm1108)* or the *fis-2(gk363)* mutation. EGL-1-induced killing, however, was significantly inhibited (approximately 40%) in the *drp-1(tm1108); fis-2(gk363)* double mutant, which is consistent with our previous observation that *drp-1(tm1108)* and *fis-2(gk363)* mutations additively reduce cell death. Similarly, expression of an activated form of CED-3 (acCED-3) under the control of the *egl-1* promoter (P_{egl-1}acCED-3) induced ectopic cell deaths and an average of 28 cell corpses in the *ced-1(e1735); ced-4(n1162)* mutant (Table 4;

Table 4. *drp-1 and fis-2* Function Downstream of, or in Parallel to, *egl-1* and *ced-3* and Independently of *cps-6* and *wah-1*

Genotype	Number of Cell Corpses			
	Mean	SEM	Range	n
N2	10.4	0.6	7–13	15
N2 (heat shock control)	10.7	0.7	7–15	15
P_{hsp}*egl-1*	40.7	2.8	25–61	15
P_{hsp}*egl-1; ced-3(n717)*	0.1	0	0–1	15
P_{hsp}*egl-1; drp-1(tm1108)*	39.7	2.3	30–64	15
P_{hsp}*egl-1; fis-2(gk363)*	38.7	1.6	35–51	15
P_{hsp}*egl-1; fis-1(tm1867); fis-2(gk363)*	37.6	2.0	31–56	15
P_{hsp}*egl-1; drp-1(tm1108); fis-2(gk363)*[a]	24.8	2.0	13–40	15
P_{egl-1}acCED-3	27.7	1.1	12–41	36
P_{egl-1}acCED-3; *drp-1(tm1108)*	27.1	0.7	18–36	33
P_{egl-1}acCED-3; *fis-2(gk363)*	28.2	1.2	11–37	31
P_{egl-1}acCED-3; *drp-1(tm1108); fis-2(gk363)*[b]	19.6	1.1	7–28	34
P_{egl-1}acCED-3; *control*(RNAi)	29.0	1.1	20–36	21
P_{egl-1}acCED-3; *cps-6*(RNAi)	28.5	0.8	19–35	24
P_{egl-1}acCED-3; *wah-1*(RNAi)	27.7	1.1	17–35	23
P_{egl-1}acCED-3; *fis-2(gk363)*; *control*(RNAi)	26.3	0.6	16–35	58
P_{egl-1}acCED-3; *fis-2(gk363)*; *cps-6*(RNAi)[c]	22.3	0.9	14–31	24
P_{egl-1}acCED-3; *fis-2(gk363)*; *wah-1*(RNAi)[d]	23.8	0.6	12-37	77
P_{egl-1}acCED-3; *drp-1(tm1108)*; *fis-2*(gk363); *control*(RNAi)	21.8	0.8	13–35	47
P_{egl-1}acCED-3; *drp-1(tm1108)*; *fis-2(gk363)*; *cps-6*(RNAi)[e]	17.0	0.7	11–26	33
P_{egl-1}acCED-3; *drp-1(tm1108)*; *fis-2(gk363)*; *wah-1*(RNAi)[f]	16.2	0.7	9–26	30

P_{hsp}*egl-1 (smls82)* is an integrated transgene containing the P_{hsp}*egl-1* constructs. EGL-1 expression was activated by heat shock treatment, and the number of cell corpses in the head region of 1.5-fold stage embryos was scored. P_{egl-1}acCED-3 (*smls111*) is an integrated transgene containing the P_{egl-1}acCED-3 construct (Kokel et al., 2006). acCED-3 is therefore expressed in cells normally destined to die. The number of cell corpses was counted in the head region of the 4-fold stage embryos. RNAi experiments were carried out as described in the Experimental Procedures. All P_{egl-1}acCED-3 strains were in the *ced-1(e1735); ced-4(n1162)* background, and results were confirmed by multiple independent blind test analyses. SEM, standard error of the mean. Unpaired two-tailed t test, compared with P_{hsp}*egl-1* animals: [a]$p = 8.7 \times 10^{-5}$; compared with P_{egl-1}acCED-3 animals: [b]$p = 1.2 \times 10^{-6}$; compared with *control*(RNAi) treatment of the same strain: [c]$p = 0.00035$, [d]$p = 0.0063$, [e]$p = 1.7 \times 10^{-5}$, and [f]$p = 1.5 \times 10^{-6}$. Others have p values > 0.05.

Kokel et al., 2006). Since the *ced-4(n1162)* mutation abolishes almost all naturally occurring cell deaths in *C. elegans* (Ellis and Horvitz, 1986), cell corpses observed in the *ced-1(e1735); ced-4(n1162)* mutant are strictly acCED-3-induced cell deaths. As in the case of EGL-1-induced cell killing, acCED-3-induced apoptosis was not affected by either the *drp-1(tm1108)* mutation or the *fis-2(gk363)* mutation (Table 4), probably because loss of either gene alone is insufficient to block acCED-3-induced cell death. However, *drp-1(tm1108); fis-2(gk363)* double mutant animals displayed a 30% reduction in acCED-3-induced cell corpses (Table 4), again consistent with previous observations that these two mutations additively inhibit cell death. The observation that *drp-1(tm1108)* and *fis-2(gk363)* mutations together inhibit both EGL-1- and acCED-3-induced cell killing to a similar degree suggests that these genes function downstream of, or in parallel to, activated CED-3 to promote cell-death execution. A role for *drp-1* and *fis-2* downstream of *ced-3* is consistent with the very weak cell-death defect observed in the *drp-1(tm1108)*, *fis-2(gk363)*, or *fis-2(tm1832)* mutant (Figure S4, Tables 1 and 2), as CED-3 likely triggers multiple cell-death execution pathways, and disruption of only one of these downstream pathways is unlikely to block cell death (Parrish et al., 2001; Wang et al., 2002).

drp-1 and *fis-2* Function Independently of the *cps-6/wah-1* DNA Degradation Pathway

A conserved aspect of apoptosis between *C. elegans* and humans is the role of apoptosis-inducing factor (AIF) and endonuclease G (*wah-1* and *cps-6* in *C. elegans*, respectively) in mediating apoptotic DNA degradation. AIF and endonuclease G reside in mitochondria of healthy cells but are released from mitochondria and translocate to the nucleus during apoptosis (Li et al., 2001; Susin et al., 1999). In *C. elegans*, CPS-6 and WAH-1 function together to promote apoptotic DNA degradation, most likely acting downstream of activated CED-3, since *cps-6* was identified as a suppressor of acCED-3-induced cell deaths and WAH-1 is released from mitochondria in a *ced-3*-dependent manner (Parrish et al., 2001; Wang et al., 2002). We thus investigated whether *drp-1* or *fis-2* might function in the CPS-6/WAH-1 mitochondrial cell-death pathway. Like the *drp-1(tm1108)* and *fis-2(gk363)* mutations, *wah-1(RNAi)* and *cps-6*(RNAi) weakly increased the number of extra cells observed in the anterior pharynx of *ced-3(n2438)* animals (Table 2; Parrish et al., 2001; Wang et al., 2002). Importantly, *wah-1*(RNAi) and *cps-6*(RNAi) also increased the number of extra cells observed in *drp-1(tm1108) ced-3(n2438)*, *ced-3(n2438); fis-2(gk363)*, and *drp-1(tm1108) ced-3(n2438); fis-2(gk363)* animals, compared with corresponding *control*(RNAi) treatment (Table 2). Moreover, *cps-6*(RNAi) or *wah-1*(RNAi) treatment of the *fis-2(gk363)* single mutant or *drp-1(tm1108); fis-2(gk363)* double mutant also resulted in stronger inhibition of acCED-3-induced cell killing than when control(RNAi) was used (Table 4). Taken together, these data suggest that *drp-1* and *fis-2* do not function in the *cps-6/wah-1* DNA degradation pathway and that these genes may act in three independent mitochondrial pathways downstream of the CED-3 caspase to facilitate execution of cell death.

CED-3 Cleaves DRP-1 In Vitro and May Activate DRP-1's Proapoptotic Function In Vivo

Given that DRP-1 and FIS-2 act downstream of the CED-3 caspase, we tested if they are CED-3 substrates. DRP-1, but not FIS-2, was cleaved by CED-3 in vitro: [^{35}S]-Methionine labeled DRP-1 was cleaved by the recombinant CED-3 protease to create a major cleavage product of approximately 67 kDa (Figure 2A and data not shown). Microsequencing of the amino terminus of this CED-3 cleavage product derived from cleavage of a recombinant DRP-1 protein revealed that proteolysis occurred between Asp^{118} and Arg^{119} (data not shown) with an adjacent tetrapeptide recognition motif (DETD) that is similar to the

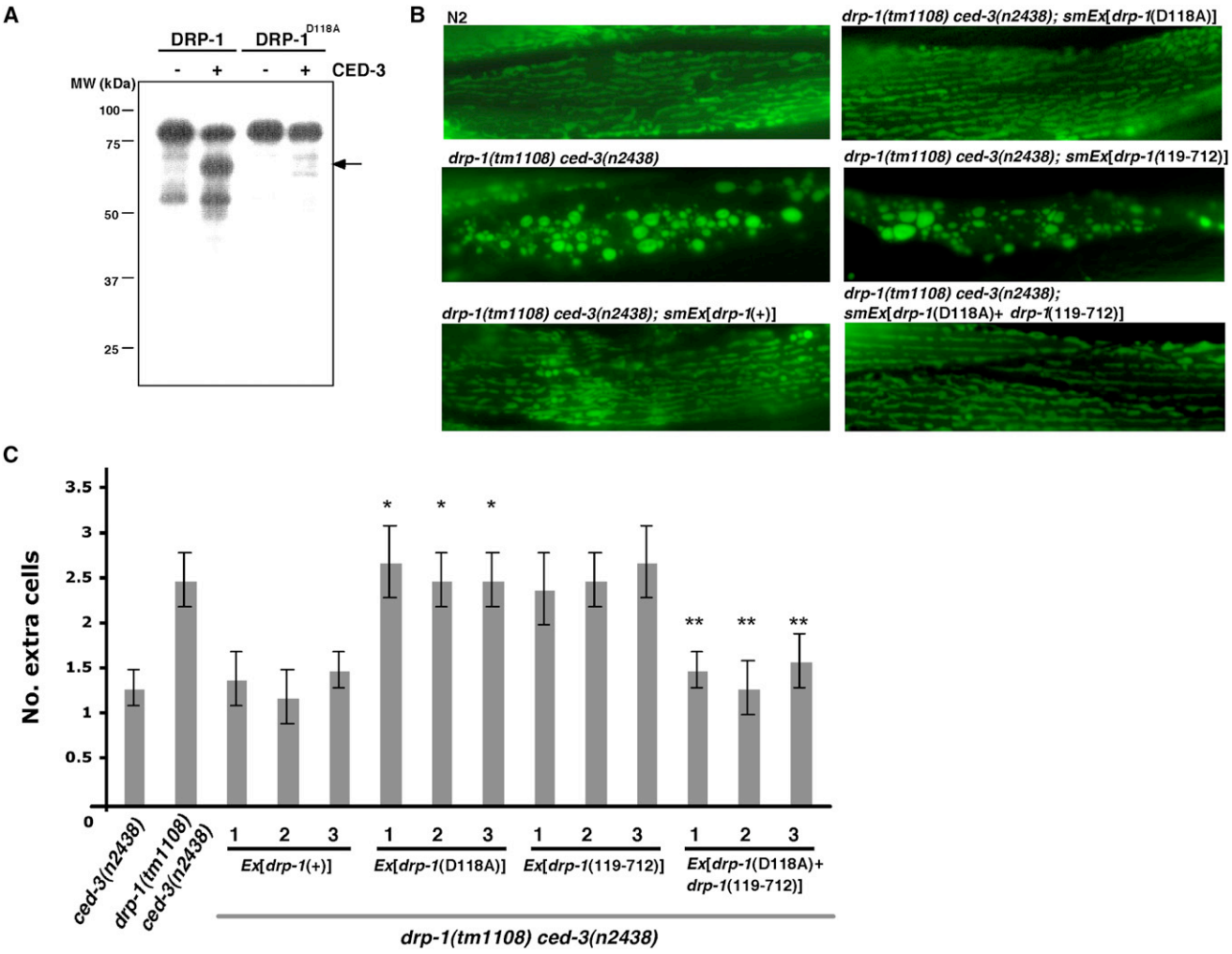

Figure 2. Cleavage of DRP-1 by CED-3 Is Important for the Proapoptotic Function of DRP-1, but Not Its Function in Regulating Mitochondria Fission

(A) DRP-1 can be cleaved by CED-3 in vitro. [^{35}S] Methionine-labeled DRP-1 or DRP-1^{D118A} was incubated with purified CED-3 protease. The 67 kDa major cleavage product is indicated by an arrow.

(B) Cleavage of DRP-1 by CED-3 is not required for its function in regulating mitochondria fission. Representative images of mitoGFP in body wall muscle cells from wild-type (N2), *drp-1(tm1108) ced-3(n2438)*, and *drp-1(tm1108) ced-3(n2438)* animals carrying transgenes with a 3994 bp *drp-1* genomic fragment [*drp-1*(+)], the *drp*-1 genomic fragment harboring the DRP-1^{D118A} mutation [drp-1*(D118A)*] or a *drp-1* construct expressing DRP-1$^{119–712}$ [*drp-1*(119–712)] under the control of the *drp-1* promoter, or transgenes containing both *drp-1*(119–712) and *drp-1*(D118A) (Supplemental Experimental Procedures).

(C) Cleavage of DRP-1 by CED-3 at Asp^{118} is important for the proapoptotic function of DRP-1 in vivo. *drp-1(tm1108) ced-3(n2438)* animals carrying the indicated transgene were analyzed for the number of extra cells in the anterior pharynx. Three independent transgenic lines were examined for each construct. Error bars indicate SEM (n = 20). Unpaired two-tailed t test, compared with *ced-3(n2438)* animals, *$p < 0.005$; compared to *drp-1(tm1108) ced-3(n2438)* animals, **$p < 0.005$.

established CED-3 recognition motif (DEXD) (Thornberry et al., 1997). A mutant DRP-1 protein carrying an Asp^{118} to Ala substitution (DRP-1^{D118A}) failed to be cleaved by CED-3 (Figure 2A), confirming that D^{118} is the major CED-3 cleavage site in DRP-1.

We then determined whether cleavage of DRP-1 by CED-3 is important for DRP-1's proapoptotic function by introducing a construct containing a 3994 bp *drp-1* genomic fragment (*drp-1*[+]) or the *drp-1* fragment carrying the CED-3-resistant DRP-1^{D118A} mutation (*drp-1*[D118A]) into *drp-1(tm1108) ced-3(n2438)* animals along with P$_{myo-3}$mitoGFP. P$_{myo-3}$mitoGFP drives the expression of mitochondrial matrix localized GFP in body wall muscle cells (Labrousse et al., 1999) and can be conveniently used to assess the rescue of the mitochondrial fission defect in *drp-1(tm1108) ced-3(n2438)* animals. As shown in Figure 2B, mitochondria in body wall muscle cells were labeled brightly by mitoGFP and appeared as connected clumps and blebs in *drp-1(tm1108) ced-3(n2438)* animals compared to the regular pattern of mitochondrial tubules observed in N2 animals. Both *drp-1*(+) and *drp-1*(D118A) transgenes completely rescued the mitochondria fission defect in *drp-1(tm1108) ced-3(n2438)* animals (Figure 2B), indicating that DRP-1^{D118A} has normal mitochondrial fission activity. However, in contrast to the *drp-1*(+)

transgene, which could rescue the enhanced cell-death defect in *drp-1(tm1108) ced-3(n2438)* animals (a mean of 2.5 extra cells) back to the level of *ced-3(n2438)* animals (a mean of 1.3 extra cells), the *drp-1*(D118A) transgene failed to do so (Figure 2C), even though DRP-1 and DRP-1^{D118A} were expressed at similar levels (Figure S9). The *drp-1*(D118A) transgene also failed to rescue the enhanced cell-death defect in *ced-4(n2273); drp-1(tm1108)* animals back to the level seen in *ced-4(n2273)* animals (Figure S10). Expression of the predicted caspase cleavage fragments of DRP-1 (DRP-1$^{1–118}$ and DRP-1$^{119–712}$) either alone or together failed to rescue the mitochondrial fission and cell-death defects in *drp-1(tm1108) ced-3(n2438)* animals (Figure 2C, Figure S11, and data not shown). However, the enhanced cell-death defect in *drp-1(tm1108) ced-3(n2438)* animals was completely rescued by coexpression of DRP-1$^{119–712}$ with DRP-1^{D118A}, even though expression of each protein alone had no rescuing activity (Figure 2C). The fact that *drp-1*(D118A) completely rescues the mitochondrial fission defect in *drp-1(tm1108) ced-3(n2438)* animals, but not the apoptosis defect caused by *drp-1(tm1108)*, and that coexpression of DRP-1$^{119–712}$ and DRP-1^{D118A} could bypass the requirement for DRP-1 cleavage in *drp-1(tm1108) ced-3(n2438)* animals, suggests that the proapoptotic function of DRP-1 is dependent on its cleavage by the CED-3 caspase and that one of the CED-3 cleavage products, DRP-1$^{119–712}$, functions with full-length DRP-1 to exert its proapoptotic effect. These results also provide direct evidence that DRP-1 acts downstream of the CED-3 caspase to promote apoptosis.

Changes in Mitochondria in Apoptotic Cells

To determine the roles of *drp-1* and *fis-2* in apoptosis, we performed EM analysis of mitochondria in apoptotic cells of *drp-1(tm1108)* and *fis-2(gk363)* embryos that also carried a *ced-1(e1735)* mutation. *ced-1(e1735)* disables cell-corpse engulfment and allows sampling of more cell corpses (Hedgecock et al., 1983). Serial EM sections through *ced-1(e1735)*, *ced-1(e1735); drp-1(tm1108)*, or *ced-1(e1735); fis-2(gk363)* 4-fold stage embryos were obtained and the mean mitochondrial length (Figure 3E), the number of mitochondria observed in cell corpses (Figure 3F), and the percentage of mitochondrial content in the cell corpses (mitochondria area index) (Figure 3G) were quantified. Living cells in *ced-1(e1735)* embryos typically had one to three large mitochondria, with a mean mitochondrial length of 0.96 μm and a 15.4% mitochondria area index (Figures 3A, 3E, 3F, and 3G). In contrast, 58% of *ced-1(e1735)* cell corpses observed in EM sections contained 1 to 2 small and spherical mitochondria (mean length 0.38 μm, Figures 3B and 3E) and 42% of them had no identifiable mitochondria at all (Figure 3F). In addition, the mitochondria area index was reduced to 8.1% in *ced-1(e1735)* cell corpses (Figure 3G). These results suggest that mitochondria are reduced or lost during apoptosis, which would eliminate cellular energy production and thus contribute to the demise of the cell (Arnoult et al., 2005; Skulachev et al., 2004). Interestingly, the mean length of remaining mitochondria in *ced-1(e1735)* cell corpses was close to the size of mitochondria in *fzo-1(tm1133)* or *eat-3(ad426)* living cells (0.38 μm and 0.44 μm, Figure 1N), again indicating that fragmentation of mitochondria per se does not cause apoptosis but, rather, is a consequence of the apoptotic cell disassembly process. In cell corpses of *ced-1(e1735); drp-1(tm1108)* embryos, we observed both large, elongated and small, spherical mitochondria (Figure 3C and Figure S12) with a mean length of 0.73 μm (Figure 3E), which is significantly shorter than that in *drp-1(tm1108)* living cells (2.28 μm, Figure 1N). This observation suggests that mitochondria breakdown or fragmentation can still occur in the *drp-1(tm1108)* apoptotic cells in the absence of the DRP-1 activity but may not proceed to completion due to the much larger size of mitochondria before the onset of apoptosis. However, there was no obvious reduction of the mitochondrial area index (14.2%) in *ced-1(e1735); drp-1(tm1108)* cell corpses. *drp-1* may therefore affect elimination of mitochondria during apoptosis. Mitochondria were small and spherical in *ced-1(e1735); fis-2(gk363)* cell corpses, with a mean length similar to that observed in *ced-1(e1735)* cell corpses (Figures 3D and 3E). However, the number of mitochondria observed in *ced-1(e1735); fis-2(gk363)* cell corpses was generally higher than in *ced-1(e1735)* corpses (Figure 3F), with fewer instances of no mitochondria observed and more instances of 2 to 3 mitochondria observed in single cross-sections of a corpse. Consistently, there was little reduction in mitochondria area index in *ced-1(e1735); fis-2(gk363)* cell corpses (Figure 3G), suggesting that *fis-2* is also involved in the removal or elimination of mitochondria from dying cells. Mitochondria in cell corpses did not appear swollen, nor did we observe rupture of the outer mitochondrial membrane or obviously remodeled cristae (Figures 3A–3D). Therefore, some of the apoptotic mitochondrial morphology transitions reported in mammals (Scorrano et al., 2002) may not occur in *C. elegans*.

DISCUSSION

Mitochondrial fission and fusion processes have recently been proposed as important mechanisms in regulating the release of mitochondrial apoptogenic factors such as cytochrome c and subsequent activation of caspases in *C. elegans*, *D. melanogaster*, and mammals (Abdelwahid et al., 2007; Frank et al., 2001; Frezza et al., 2006; Goyal et al., 2007; Jagasia et al., 2005; James et al., 2003; Karbowski et al., 2002, 2004; Lee et al., 2004; Sugioka et al., 2004). However, a comprehensive genetic analysis of the roles of mitochondrial dynamin genes in apoptosis has not been reported. Using live imaging and high-resolution electron microscopy, we show that mitochondria are constitutively fragmented in *C. elegans* animals deficient in the profusion genes *fzo-1* and *eat-3* and that normal cristae structure is lost in the *eat-3* mutant. However, no excess cell death is observed in these mutants, despite the fact that mitochondria in living cells of these animals are of a similar size to those observed in apoptotic cells (Figure 1N and Figure 3E). On the other hand, in the *drp-1(tm1108)* strong loss-of-function mutant, mitochondria are fused together into a long, connected network, yet programmed cell death appears to occur normally, although a mild cell-death defect could be detected in sensitized genetic backgrounds. These observations argue against a casual relationship between the connectivity of the mitochondrial network and the extent of programmed cell death and the hypothesis that the mitochondrial fission process activates apoptosis in *C. elegans*.

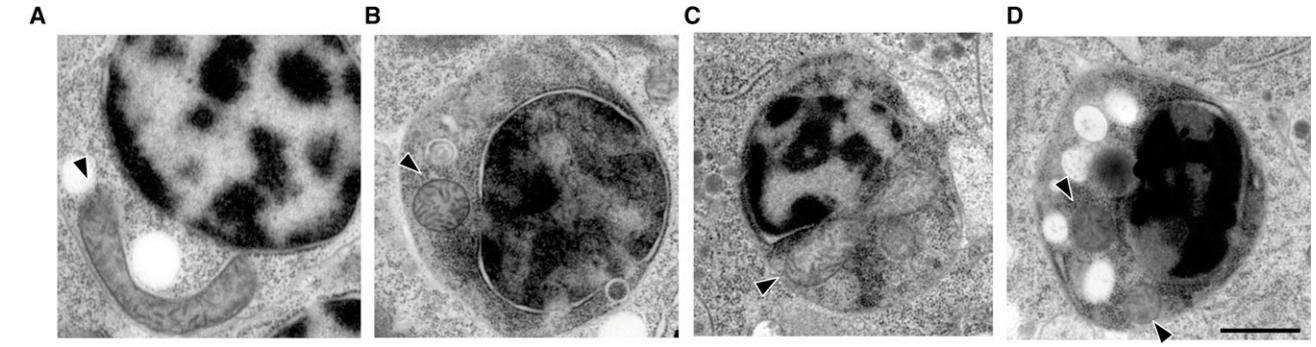

E

genotype	mito length (μm)	s.e.m.	range	n
ced-1(e1735) live cells	0.96	0.08	0.36-1.90	33
ced-1(e1735) corpses	0.38	0.03	0.21-0.71	28
ced-1(e1735); drp-1(tm1108) corpses	0.73	0.08	0.19-1.89	27
ced-1(e1735); fis-2(gk363) corpses	0.38	0.03	0.14-0.94	35

G

genotype	mito area index (%)	s.e.m.	range	n
ced-1(e1735) live cells	15.4 [1]	2.0	3.6-32.4	14
ced-1(e1735) corpses	8.1	0.7	3.4-11.4	19
ced-1(e1735); drp-1(tm1108) corpses	14.2 [2]	1.8	5.9-30.3	20
ced-1(e1735); fis-2(gk363) corpses	12.9 [3]	1.9	2.7-33.4	14

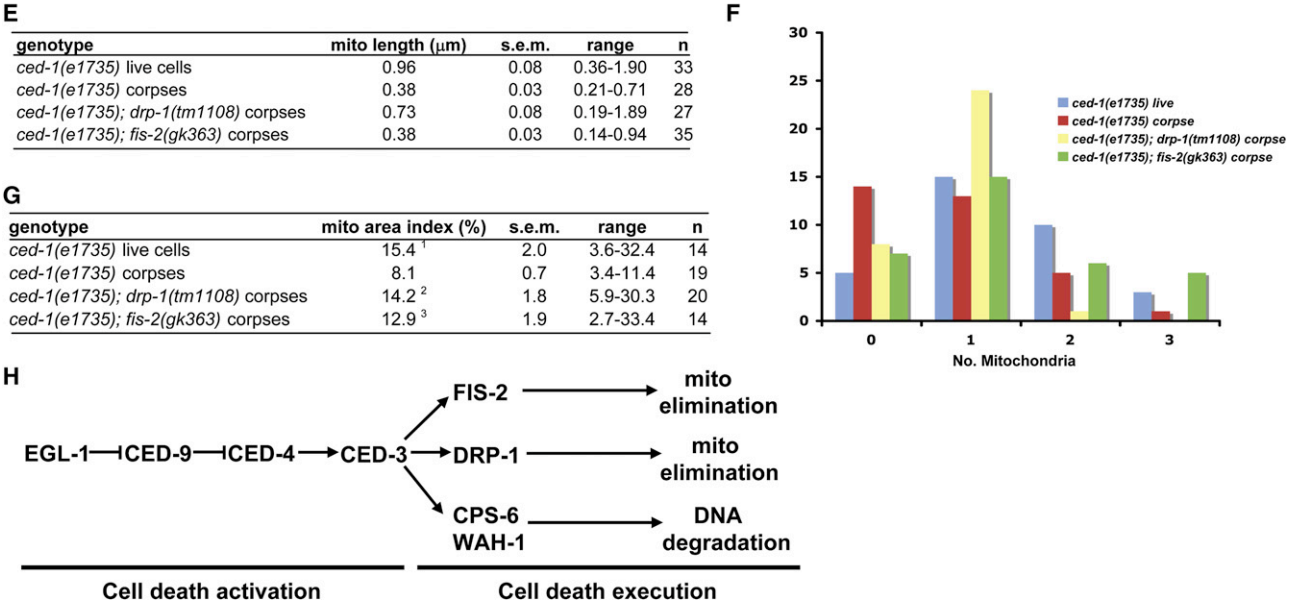

Figure 3. Electron Microscopy Analysis of Mitochondria in Cell Corpses of *drp-1* and *fis-2* Mutants

(A–D) Representative EM micrographs from serial sections of *ced-1(e1735)* living cells (A), cell corpses in *ced-1(e1735)* (B), *ced-1(e1735); drp-1(tm1108)* (C), and *ced-1(e1735); fis-2(gk363)* (D) 4-fold stage embryos are shown. Arrowheads denote the longitudinal axis of mitochondria. Compared with small, spherical mitochondria seen in *ced-1(e1735)* and *ced-1(e1735); fis-2(gk363)* corpses, some larger, elongated mitochondria are seen in the *ced-1(e1735); drp-1(tm1108)* cell corpses. Scale bar represents 0.5 μm.

(E) Quantification of the mitochondrial length in cell corpses. The mean mitochondria length, range of mitochondria length, and standard error of the mean (SEM) are shown. n indicates the number of mitochondria scored.

(F) Quantification of the number of mitochondria in cell corpses. Randomly chosen EM sections of *ced-1(e1735)* living cells or cell corpses in the indicated mutant embryos were analyzed, and the number of mitochondria in each section was counted (n = 33). Data are shown as the number of cells or cell corpses (y axis) containing a particular number of mitochondria (x axis).

(G) Comparison of the mitochondrial area index. The mitochondrial area index represents the percentage of total mitochondria content within the whole cell. The mean mitochondrial area index, the range of the index, the standard error of the mean (SEM), and the number of corpses scored (n) are shown. Unpaired two-tailed t test, compared with *ced-1(e1735)* cell corpses, $^{1}p = 4.4 \times 10^{-4}$, $^{2}p = 7.6 \times 10^{-4}$, and $^{3}p = 1.1 \times 10^{-2}$.

(H) A model for programmed cell death in *C. elegans*. In cells programmed to die, EGL-1 antagonizes the CED-4-inhibitory activity of CED-9, allowing CED-4 to activate the CED-3 zymogen. Activated CED-3 triggers three independent cell-death pathways derived from the mitochondrion, mediated by DRP-1, FIS-2, and CPS-6/WAH-1. Cleavage of DRP-1 by CED-3 is important for DRP-1's proapoptotic function, which may contribute to the removal of mitochondria. FIS-2 may also independently promote the elimination of mitochondria from dying cells. The release of CPS-6 and WAH-1 from mitochondria and translocation to the nucleus triggers apoptotic DNA degradation (Parrish et al., 2001; Wang et al., 2002).

Our study reaches a different conclusion from a previous report (Jagasia et al., 2005), which suggested that DRP-1-mediated mitochondrial fission functions upstream of caspase activation in *C. elegans*. The different conclusions could be attributed to the different methods used to inactivate the *drp-1* gene. Our finding was based on analysis of the *drp-1* null mutant, whereas the other study was based on analysis of animals overexpressing a dominant-negative DRP-1(K40A) mutant. However, we found that overexpression of DRP-1(K40A) still inhibits apoptosis in *drp-1(tm1108)* animals that have no endogenous *drp-1* protein and have no cell-death defect on its own (Table S1), suggesting that DRP-1(K40A) may have an off-target effect on apoptosis. Furthermore, we found that overexpression of *drp-1* failed to induce ectopic apoptosis (Table S2), which is consistent with the

findings that cleavage of DRP-1 by CED-3 could be important for activating DRP-1's proapoptotic function and that ectopic apoptosis is not observed in either *fzo-1(tm1133)* or *eat-3(ad426)* animals (Figure S4), where mitochondria are highly fragmented. These findings underscore the need to study mitochondrial dynamins in a physiological context.

In mammals, the profusion protein OPA1 forms oligomers that maintain tight cristae junctions, preventing release of cytochrome c from cristae folds until cells are committed to die (Cipolat et al., 2006; Frezza et al., 2006). This OPA1 checkpoint does not appear to exist in the worm, possibly because CED-4 can directly activate the CED-3 zymogen independent of cytochrome c or other mitochondrial factors (Yan et al., 2005). DRP1-mediated mitochondrial fission has been proposed to be an important cellular event that occurs upstream of cytochrome c release and caspase activation in mammals (Frank et al., 2001) and an event that may activate the CED-3 caspase in *C. elegans* via a mechanism dependent on a unique *ced-9* cell killing activity (Jagasia et al., 2005). However, this proposed *ced-9*-dependent, caspase-activating role by DRP-1-mediated mitochondria fission is contradicted by the following findings: (1) *drp-1* promotes apoptosis independent of *ced-9* in *C. elegans* (strong loss-of-function *drp-1* and *ced-9* mutations additively cause defects in cell death; Table 3); (2) *drp-1* genetically acts downstream of the *ced-3* caspase (Table 4), and DRP-1 can be cleaved by the CED-3 caspase; and (3) the CED-3-resistant DRP-1^{D118A} mutant has normal mitochondrial fission function but is defective in its proapoptotic function (Figure 2), providing strong evidence that DRP-1 and mitochondria fission do not regulate CED-3 activation. Instead, we propose that CED-9 functions at an early step to regulate caspase activation by preventing the formation of CED-4 oligomers needed for CED-3 activation (Chinnaiyan et al., 1997; Conradt and Horvitz, 1998; Parrish et al., 2000; Yan et al., 2005), whereas *drp-1* and other genes such as *fis-2* and *cps-6/wah-1* act late in the apoptosis program, after the CED-3 caspase is already activated, to independently mediate various important cell-death execution events, including removal of mitochondria and fragmentation of chromosomes (Figure 3H), all of which concertedly facilitate the demise of a cell.

The downstream cell dismantling pathways mediated by *drp-1*, *fis-2*, and *cps-6/wah-1* may be conserved between *C. elegans* and mammals. Indeed, CPS-6/endoG and WAH-1/AIF are conserved regulators of the apoptotic DNA degradation event (Susin et al., 1999; Parrish et al., 2001; Li et al., 2001; Wang et al., 2002), and mitochondrial release of AIF and WAH-1 appears to occur after caspase activation in both *C. elegans* and mammalian apoptosis (Wang et al., 2002; Arnoult et al., 2003; Lakhani et al., 2006). In *C. elegans*, CED-3 could cleave a fraction of DRP-1, leading to the formation of DRP-1 complexes containing both full-length DRP-1 and DRP-$1^{119–712}$, which may redirect DRP-1 activity toward apoptotic mitochondrial elimination. Thus, the primordial apoptotic role for *drp-1* may be to eliminate mitochondria after caspase activation, although Drp1 may have evolved an additional apoptotic role in mediating the release of cytochrome c from mitochondria in mammals (Cassidy-Stone et al., 2008; Frank et al., 2001). Altogether, our findings underscore an important role of mitochondria in the cell disassembly processes rather than the activation of apoptosis in *C. elegans*.

EXPERIMENTAL PROCEDURES

Counting of Cell Corpses and Extra Cells

The number of cell corpses in the head region of living embryos or L1 larvae and the number of extra surviving cells in the anterior pharynx of L4 larvae were determined as described previously (Hengartner et al., 1992; Stanfield and Horvitz, 2000). Statistical analysis was preformed using Microsoft Excel 2004 software.

DRP-1 Antibody

cDNA fragments encoding the full-length or the first 270 residues of DRP-1 were subcloned into the pGEX-4T-3 vector (Amersham Biosciences) and expressed in *E. coli* BL21 strain. Recombinant GST-DRP-1 proteins were purified from the soluble fraction of the bacterial lysates using Glutathione Sepharose 4B beads (GE Healthcare). Rats were immunized with a mixture of purified GST-DRP-1 and GST-DRP-1(1–270) proteins and terminal bleeds were affinity purified against GST-DRP-1(1–270) as previously described (Wang et al., 2007).

CED-3 Cleavage Assay

One microliter of [^{35}S] Methionine-labeled DRP-1 and DRP-1^{D118A} (TNT Reticulocyte Lysate, Promega) was incubated with 5 ng of recombinant CED-3 protein in 10 μl of CED-3 buffer (50 mM Tris HCl [pH 8.0], 0.5 mM EDTA, 0.5 mM sucrose, and 5% glycerol) at 37°C for 2 hr. The reactions were terminated by the addition of SDS gel loading buffer, resolved on a 10% SDS-PAGE gel, and subjected to autoradiography.

Live Imaging of *C. elegans* Mitochondria and Electron Microscopy

Labeling of mitochondria with tetramethylrhodamine ester (TMRE; Molecular Probes) was carried out as previously described (Jagasia et al., 2005). Imaging of MitoGFP in body wall muscle cells was done as described previously (Labrousse et al., 1999). Detailed protocols for visualization of mitochondria by electron microscopy and quantification of mitochondrial length, mitochondria number in cell corpses, and mitochondrial area index are described in the Supplemental Data.

SUPPLEMENTAL DATA

The Supplemental Data include Supplemental Experimental Procedures, 12 figures, and two tables and can be found with this article online at http://www.molcecule.org/cgi/content/full/31/4/586/DC1/.

ACKNOWLEDGMENTS

We thank E. Griffiths and D. William for technical assistance, T. Blumenthal and members of the Xue lab for comments and discussions, *Caenorhabditis* Genetics Center for strains, and Y. Kohara for *drp-1* and *fis-2* cDNAs. This research was supported by fellowships from the Jane Coffin Child Memorial Fund for Medical Research (D.G.B.) and the Canadian Institutes of Health Research (D.G.B.), the Burroughs Wellcome Fund Career Award (D.X.), and the NIH R01 GM059083 and GM079097 grants (D.X.).

Received: January 18, 2008
Revised: May 12, 2008
Accepted: July 28, 2008
Published: August 21, 2008

REFERENCES

Abdelwahid, E., Yokokura, T., Krieser, R.J., Balasundaram, S., Fowle, W.H., and White, K. (2007). Mitochondrial disruption in *Drosophila* apoptosis. Dev. Cell *12*, 793–806.

Alirol, E., James, D., Huber, D., Marchetto, A., Vergani, L., Martinou, J.C., and Scorrano, L. (2006). The mitochondrial fission protein hFis1 requires the endoplasmic reticulum gateway to induce apoptosis. Mol. Biol. Cell *17*, 4593–4605.

Antignani, A., and Youle, R.J. (2006). How do Bax and Bak lead to permeabilization of the outer mitochondrial membrane? Curr. Opin. Cell Biol. *18*, 685–689.

Arnoult, D., Karbowski, M., and Youle, R.J. (2003). Caspase inhibition prevents the mitochondrial release of apoptosis-inducing factor. Cell Death Differ. *10*, 845–849.

Arnoult, D., Rismanchi, N., Grodet, A., Roberts, R.G., Seeburg, D.P., Estaquier, J., Sheng, M., and Blackstone, C. (2005). Bax/Bak-dependent release of DDP/TIMM8a promotes Drp1-mediated mitochondrial fission and mitoptosis during programmed cell death. Curr. Biol. *15*, 2112–2118.

Avery, L. (1993). The genetics of feeding in *Caenorhabditis elegans*. Genetics *133*, 897–917.

Bleazard, W., McCaffery, J.M., King, E.J., Bale, S., Mozdy, A., Tieu, Q., Nunnari, J., and Shaw, J.M. (1999). The dynamin-related GTPase Dnm1 regulates mitochondrial fission in yeast. Nat. Cell Biol. *1*, 298–304.

Bloss, T.A., Witze, E.S., and Rothman, J.H. (2003). Suppression of CED-3-independent apoptosis by mitochondrial betaNAC in *Caenorhabditis elegans*. Nature *424*, 1066–1071.

Cassidy-Stone, A., Chipuk, J.E., Ingerman, E., Song, C., Yoo, C., Kuwana, T., Kurth, M.J., Shaw, J.T., Hinshaw, J.E., Green, D.R., and Nunnari, J. (2008). Chemical inhibition of the mitochondrial division dynamin reveals its role in Bax/Bak-dependent mitochondrial outer membrane permeabilization. Dev. Cell *14*, 193–204.

Cereghetti, G.M., and Scorrano, L. (2006). The many shapes of mitochondrial death. Oncogene *25*, 4717–4724.

Chan, D.C. (2006). Mitochondrial fusion and fission in mammals. Annu. Rev. Cell Dev. Biol. *22*, 79–99.

Chinnaiyan, A.M., O'Rourke, K., Lane, B.R., and Dixit, V.M. (1997). Interaction of CED-4 with CED-3 and CED-9: a molecular framework for cell death. Science *275*, 1122–1126.

Cipolat, S., Rudka, T., Hartmann, D., Costa, V., Serneels, L., Craessaerts, K., Metzger, K., Frezza, C., Annaert, W., D'Adamio, L., et al. (2006). Mitochondrial rhomboid PARL regulates cytochrome c release during apoptosis via OPA1-dependent cristae remodeling. Cell *126*, 163–175.

Conradt, B., and Horvitz, H.R. (1998). The *C. elegans* protein EGL-1 is required for programmed cell death and interacts with the Bcl-2-like protein CED-9. Cell *93*, 519–529.

Delivani, P., Adrain, C., Taylor, R.C., Duriez, P.J., and Martin, S.J. (2006). Role for CED-9 and Egl-1 as regulators of mitochondrial fission and fusion dynamics. Mol. Cell *21*, 761–773.

Ellis, H.M., and Horvitz, H.R. (1986). Genetic control of programmed cell death in the nematode *C. elegans*. Cell *44*, 817–829.

Ellis, R.E., Jacobson, D.M., and Horvitz, H.R. (1991). Genes required for the engulfment of cell corpses during programmed cell death in *Caenorhabditis elegans*. Genetics *129*, 79–94.

Estaquier, J., and Arnoult, D. (2007). Inhibiting Drp1-mediated mitochondrial fission selectively prevents the release of cytochrome c during apoptosis. Cell Death Differ. *14*, 1086–1094.

Fannjiang, Y., Cheng, W.C., Lee, S.J., Qi, B., Pevsner, J., McCaffery, J.M., Hill, R.B., Basanez, G., and Hardwick, J.M. (2004). Mitochondrial fission proteins regulate programmed cell death in yeast. Genes Dev. *18*, 2785–2797.

Frank, S., Gaume, B., Bergmann-Leitner, E.S., Leitner, W.W., Robert, E.G., Catez, F., Smith, C.L., and Youle, R.J. (2001). The role of dynamin-related protein 1, a mediator of mitochondrial fission, in apoptosis. Dev. Cell *1*, 515–525.

Frezza, C., Cipolat, S., Martins de Brito, O., Micaroni, M., Beznoussenko, G.V., Rudka, T., Bartoli, D., Polishuck, R.S., Danial, N.N., De Strooper, B., and Scorrano, L. (2006). OPA1 controls apoptotic cristae remodeling independently from mitochondrial fusion. Cell *126*, 177–189.

Goyal, G., Fell, B., Sarin, A., Youle, R.J., and Sriram, V. (2007). Role of mitochondrial remodeling in programmed cell death in *Drosophila melanogaster*. Dev. Cell *12*, 807–816.

Hedgecock, E.M., Sulston, J.E., and Thomson, J.N. (1983). Mutations affecting programmed cell deaths in the nematode *Caenorhabditis elegans*. Science *220*, 1277–1279.

Hengartner, M.O., and Horvitz, H.R. (1994). Activation of *C. elegans* cell death protein CED-9 by an amino-acid substitution in a domain conserved in Bcl-2. Nature *369*, 318–320.

Hengartner, M.O., Ellis, R.E., and Horvitz, H.R. (1992). *Caenorhabditis elegans* gene ced-9 protects cells from programmed cell death. Nature *356*, 494–499.

Horvitz, H.R. (1999). Genetic control of programmed cell death in the nematode *Caenorhabditis elegans*. Cancer Res. *59*, 1701s–1706s.

Jagasia, R., Grote, P., Westermann, B., and Conradt, B. (2005). DRP-1-mediated mitochondrial fragmentation during EGL-1-induced cell death in *C. elegans*. Nature *433*, 754–760.

James, D.I., Parone, P.A., Mattenberger, Y., and Martinou, J.C. (2003). hFis1, a novel component of the mammalian mitochondrial fission machinery. J. Biol. Chem. *278*, 36373–36379.

Karbowski, M., Lee, Y.J., Gaume, B., Jeong, S.Y., Frank, S., Nechushtan, A., Santel, A., Fuller, M., Smith, C.L., and Youle, R.J. (2002). Spatial and temporal association of Bax with mitochondrial fission sites, Drp1, and Mfn2 during apoptosis. J. Cell Biol. *159*, 931–938.

Karbowski, M., Arnoult, D., Chen, H., Chan, D.C., Smith, C.L., and Youle, R.J. (2004). Quantitation of mitochondrial dynamics by photolabeling of individual organelles shows that mitochondrial fusion is blocked during the Bax activation phase of apoptosis. J. Cell Biol. *164*, 493–499.

Kokel, D., Li, Y., Qin, J., and Xue, D. (2006). The nongenotoxic carcinogens naphthalene and para-dichlorobenzene suppress apoptosis in *Caenorhabditis elegans*. Nat. Chem. Biol. *2*, 338–345.

Labrousse, A.M., Zappaterra, M.D., Rube, D.A., and van der Bliek, A.M. (1999). *C. elegans* dynamin-related protein DRP-1 controls severing of the mitochondrial outer membrane. Mol. Cell *4*, 815–826.

Lakhani, S.A., Masud, A., Kuida, K., Porter, G.A., Jr., Booth, C.J., Mehal, W.Z., Inayat, I., and Flavell, R.A. (2006). Caspases 3 and 7: key mediators of mitochondrial events of apoptosis. Science *311*, 847–851.

Lee, Y.J., Jeong, S.Y., Karbowski, M., Smith, C.L., and Youle, R.J. (2004). Roles of the mammalian mitochondrial fission and fusion mediators Fis1, Drp1, and Opa1 in apoptosis. Mol. Biol. Cell *15*, 5001–5011.

Li, L.Y., Luo, X., and Wang, X. (2001). Endonuclease G is an apoptotic DNase when released from mitochondria. Nature *412*, 95–99.

Mozdy, A.D., McCaffery, J.M., and Shaw, J.M. (2000). Dnm1p GTPase-mediated mitochondrial fission is a multi-step process requiring the novel integral membrane component Fis1p. J. Cell Biol. *151*, 367–380.

Okamoto, K., and Shaw, J.M. (2005). Mitochondrial morphology and dynamics in yeast and multicellular eukaryotes. Annu. Rev. Genet. *39*, 503–536.

Parone, P.A., and Martinou, J.C. (2006). Mitochondrial fission and apoptosis: an ongoing trial. Biochim. Biophys. Acta *1763*, 522–530.

Parone, P.A., James, D.I., Da Cruz, S., Mattenberger, Y., Donze, O., Barja, F., and Martinou, J.C. (2006). Inhibiting the mitochondrial fission machinery does not prevent Bax/Bak-dependent apoptosis. Mol. Cell. Biol. *26*, 7397–7408.

Parrish, J., Li, L., Klotz, K., Ledwich, D., Wang, X., and Xue, D. (2001). Mitochondrial endonuclease G is important for apoptosis in *C. elegans*. Nature *412*, 90–94.

Parrish, J., Metters, H., Chen, L., and Xue, D. (2000). Demonstration of the in vivo interaction of key cell death regulators by structure-based design of second-site suppressors. Proc. Natl. Acad. Sci. USA *97*, 11916–11921.

Reddien, P.W., and Horvitz, H.R. (2004). The engulfment process of programmed cell death in *caenorhabditis elegans*. Annu. Rev. Cell Dev. Biol. *20*, 193–221.

Reinke, V., Gil, I.S., Ward, S., and Kazmer, K. (2004). Genome-wide germline-enriched and sex-biased expression profiles in *Caenorhabditis elegans*. Development *131*, 311–323.

Scorrano, L., Ashiya, M., Buttle, K., Weiler, S., Oakes, S.A., Mannella, C.A., and Korsmeyer, S.J. (2002). A distinct pathway remodels mitochondrial cristae and mobilizes cytochrome c during apoptosis. Dev. Cell *2*, 55–67.

Skulachev, V.P., Bakeeva, L.E., Chernyak, B.V., Domnina, L.V., Minin, A.A., Pletjushkina, O.Y., Saprunova, V.B., Skulachev, I.V., Tsyplenkova, V.G., Vasiliev, J.M., et al. (2004). Thread-grain transition of mitochondrial reticulum as a step of mitoptosis and apoptosis. Mol. Cell. Biochem. *256–257*, 341–358.

Stanfield, G.M., and Horvitz, H.R. (2000). The ced-8 gene controls the timing of programmed cell deaths in *C. elegans*. Mol. Cell *5*, 423–433.

Sugioka, R., Shimizu, S., and Tsujimoto, Y. (2004). Fzo1, a protein involved in mitochondrial fusion, inhibits apoptosis. J. Biol. Chem. *279*, 52726–52734.

Susin, S.A., Lorenzo, H.K., Zamzami, N., Marzo, I., Snow, B.E., Brothers, G.M., Mangion, J., Jacotot, E., Costantini, P., Loeffler, M., et al. (1999). Molecular characterization of mitochondrial apoptosis-inducing factor. Nature *397*, 441–446.

Thornberry, N.A., Rano, T.A., Peterson, E.P., Rasper, D.M., Timkey, T., Garcia-Calvo, M., Houtzager, V.M., Nordstrom, P.A., Roy, S., Vaillancourt, J.P., et al. (1997). A combinatorial approach defines specificities of members of the caspase family and granzyme B. Functional relationships established for key mediators of apoptosis. J. Biol. Chem. *272*, 17907–17911.

Wang, X., Yang, C., Chai, J., Shi, Y., and Xue, D. (2002). Mechanisms of AIF-mediated apoptotic DNA degradation in *Caenorhabditis elegans*. Science *298*, 1587–1592.

Wang, X., Wang, J., Gengyo-Ando, K., Gu, L., Sun, C.L., Yang, C., Shi, Y., Kobayashi, T., Shi, Y., Mitani, S., et al. (2007). *C. elegans* mitochondrial factor WAH-1 promotes phosphatidylserine externalization in apoptotic cells through phospholipid scramblase SCRM-1. Nat. Cell Biol. *9*, 541–549.

Yan, N., Chai, J., Lee, E.S., Gu, L., Liu, Q., He, J., Wu, J.W., Kokel, D., Li, H., Hao, Q., et al. (2005). Structure of the CED-4-CED-9 complex provides insights into programmed cell death in *Caenorhabditis elegans*. Nature *437*, 831–837.

Yan, N., Xu, Y., and Shi, Y. (2006). 2:1 Stoichiometry of the CED-4-CED-9 complex and the tetrameric CED-4: insights into the regulation of CED-3 activation. Cell Cycle *5*, 31–34.

Youle, R.J., and Karbowski, M. (2005). Mitochondrial fission in apoptosis. Nat. Rev. Mol. Cell Biol. *6*, 657–663.

Yu, T., Fox, R.J., Burwell, L.S., and Yoon, Y. (2005). Regulation of mitochondrial fission and apoptosis by the mitochondrial outer membrane protein hFis1. J. Cell Sci. *118*, 4141–4151.

Molecular Cell, Volume *31*

Supplemental Data

Caenorhabditis elegans drp-1 and *fis-2* Regulate Distinct Cell Death Execution Pathways Downstream of *ced-3* and Independent of *ced-9*

David G. Breckenridge, Byung-Ho Kang, David Kokel, Shohei Mitani, L. Andrew Staehelin, and Ding Xue

Supplemental Experimental Procedures

Strains and culture conditions

Strains of *C. elegans* were maintained at 20°C using standard protocols (Brenner, 1974). *N2* was the wild type stain. Alleles of *ced-3*, *ced-4* and *ced-9* used in this study have been described previously (1997). *eat-3(ad426)* and *fis-2(gk363)* mutants were obtained from *Caenorhabditis* Genetics Center (CGC) (Avery, 1993). *eat-3(tm1107)*, *fzo-1(tm1133)*, *drp-1(tm1108)*, *fis-1(tm1867)*, *fis-1(tm2227)*, and *fis-2(tm1832)* animals were obtained from Japan National Bioresource Project (NBRP). All strains were backcrossed with *N2* animals 5-10 times prior to analysis. *cps-6* and *wah-1* RNAi treatment was carried out using a bacterial feeding protocol as previously described (Kamath et al., 2001; Wang et al., 2002). Animals were subjected to two generations of RNAi treatment and F2 progeny were scored for the cell death defects.

Molecular Biology

P_{hsp}*egl-l*, P_{hsp} *drp-1*, and P_{hsp}*fis-2* expression vectors were constructed by subcloning the respective full-length cDNAs into the pPD49.78 and pPD49.83 vectors, which harbor the *C. elegans hsp-16.2* and *hsp-16.41* promoters, respectively. To construct P_{hsp}*gfp::fis-2*, a

coding region for the Green Fluorescent Protein (GFP) was amplified from the pPD95.79 vector and subcloned into the pPD49.78 and pPD49.83 vectors, creating pPD49.78-GFP and pPD49.83-GFP constructs. Full-length *fis-2* cDNA was then subcloned into the pPD49.78-GFP and pPD49.83-GFP vectors as a carboxyl terminal fusion to GFP. *drp-1* cDNA was amplified by polymerase chain reaction (PCR) from a *C. elegans* cDNA library and cloned into the pDONR221 donor and the pDEST14 destination gateway vectors according to the manufacturers protocols (Invitrogen). The 3994 bp *drp-1* genomic rescuing construct (containing 963 bp of sequence upstream of the initiation ATG codon and 479 bp downstream of the termination codon) was amplified by PCR from the fosmid clone wrm0628dc05 and cloned into pDONR221, creating the pENTR-*drp-1*(+) construct. Constructs containing the D118A mutation were created using standard site-directed mutagenesis techniques. PCR amplification and the gateway cloning method were used to create a gateway entry vector containing *drp-1*(119-712), pENTR-*drp-1*(119-712), which also includes introns and 479 bp of sequence after the termination codon. *drp-1*(119-712) was then placed under the control of the 963 bp *drp-1* promoter by performing an LR reaction between pENTR-*drp-1*(119-712) and a P_{drp-1}DEST vector.

Transgenic Animals

Plasmids (2-25 µg/ml) were injected into *unc-76(e911),* N2, *drp-1(tm1108) ced-3(n2438), or ced-4(n2273); drp-1(tm1108)* animals with p76-16B (25 µg/ml), a construct that rescues the *unc-76(e991)* mutant, or with pRF4 (25 µg/ml), a dominant *rol-6* construct, or with P_{myo-3}MitoGFP (Labrousse et al., 1999) as co-injection markers. For the

rescuing experiments with *drp-1(tm1108) ced-3(n2438)* animals, *drp-1*(+) or *drp-1*(D118A) constructs were injected at 10 µg/ml, while *drp-1*(D118A) and *drp-1*(119-712) constructs were co-injected at 10 µg/ml and 2 µg/ml, respectively. Stable transgenic lines of non-Unc animals, Roller animals, or GFP transgenic animals were then selected. An integrated line containing the P_{hsp}*egl-1* constructs (*smIs82*) or the P_{egl-1}acCED-3 construct (*smIs111)* was obtained by irradiating the animals with the corresponding extrachromosomal arrays with gamma rays and screening for progeny with 100% inheritance of the transgene. Integrants were backcrossed with N2 animals five times prior to crossing into the various mitochondrial fission and fusion mutants. For the heat-shock experiments, heat-shock treatment of animals was carried out as previously described (Jagasia et al., 2005) and the number of cell corpses at the 1.5-fold stage embryos was counted 2-3 hours post the heat-shock treatment.

Live imaging of *C. elegans* mitochondria and electron microscopy

Labeling of mitochondria with tetramethylrhodamine ester (TMRE; Molecular Probes) was carried out as previously described (Jagasia et al., 2005). Embryos were dissected from gravid adults on a 2% agar pad soaked in M9 buffer and visualized using an Axioplan 2 Nomarski Microscope (Carl Zeiss MicroImaging Inc., Thorton, NY, USA) equipped with a SensiCam CCD camera and slidebook 4.0 software (Intelligent Imaging Innovations, Denver, CO, USA). Imaging MitoGFP in body wall muscle cells was done as described previously (Labrousse et al., 1999). For visualization of mitochondria by electron microscopy, adult worms were mixed with *E. coli* and loaded into type B high-pressure freezing planchettes (Baltec, Tucson, AZ). After cryofixed by Baltec HPM010

high-pressure freezer, the samples were freeze-substituted in anhydrous acetone containing 2% osmium tetroxide at –80^{o}C for 4 days and slowly warmed to room temperature over 48 hours. Infiltration with EPON/Araldite resin (Ted Pella, Reddings, CA), mounting, sectioning, and post-staining were performed essentially as described (Muller-Reichert et al., 2003). Worms and embryos were observed with a Philips (Hillsboro, OR) CM10 electron microscope operated at 80 kV. To prepare 4-fold stage embryos for EM sectioning, adult hermaphrodite animals were starved 5-6 hours prior to fixation so that embryos could mature and accumulate in the uterus of animals. Quantification of EM sections was preformed with Image J software. Mitochondrial length was estimated by measuring the longest longitudinal axis of randomly selected mitochondria. For each strain, mitochondria were selected from over 10 different embryos inside at least two thin-sectioned gravid adult animals. The mean length of mitochondria in *drp-1(tm1108)* animals is likely to be highly underestimated because as the length of an individual mitochondrion increases, the chance of capturing the entire organelle in a single thin sectioned plane decreases. In cases where serial sectioning was employed, the section in which a given mitochondria appeared largest was chosen for measurement. To quantify mitochondria in cell corpses, a single section through each cell corpse was chosen at random and the number of individual mitochondria in that section was counted. This method was adopted instead of quantifying the total number of mitochondria observed in serial sections through a cell corpse, because it rules out bias that may be attained if a series of sections does not go completely through a cell corpse and allows a greater sampling number. To obtain the mitochondrial area index, serial sections through a cell corpse were analyzed and the sections where each mitochondrion

appeared largest were chosen for area measurement. The areas of each mitochondrion measured in a cell corpse were added and then divided by the total area of the corpse (measured from the section where the corpse area appeared largest).

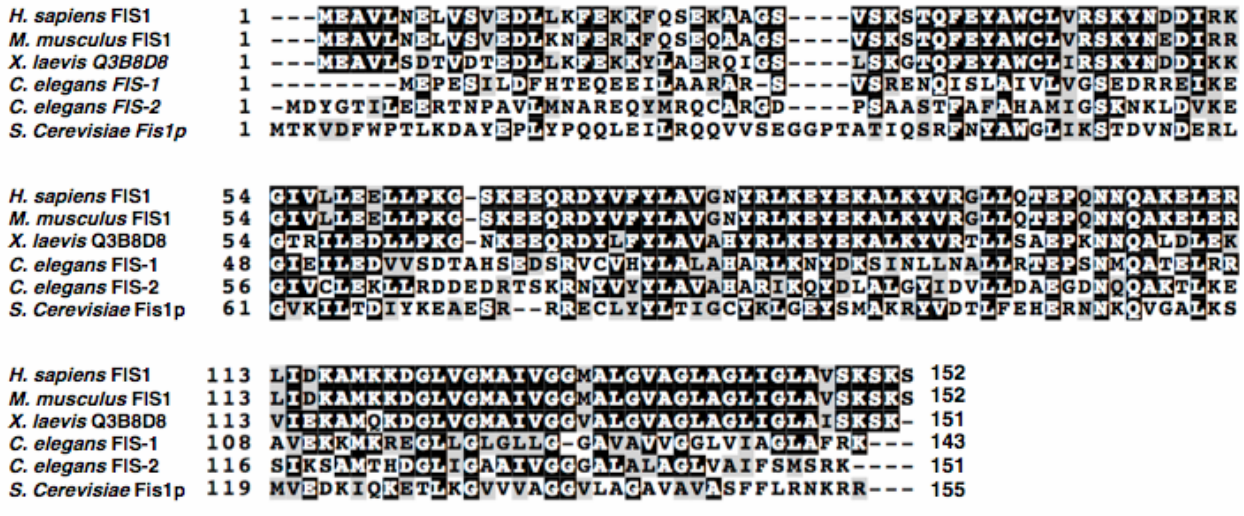

Figure S1. Alignment of Fis genes from human, mouse, *X. laevis*, *C. elegans*, and *S. cerevisiae*. Sequences were aligned and shaded using the ClustalW and BoxShade programs, respectively. Identical residues are shaded in black and conserved residues are shaded in grey.

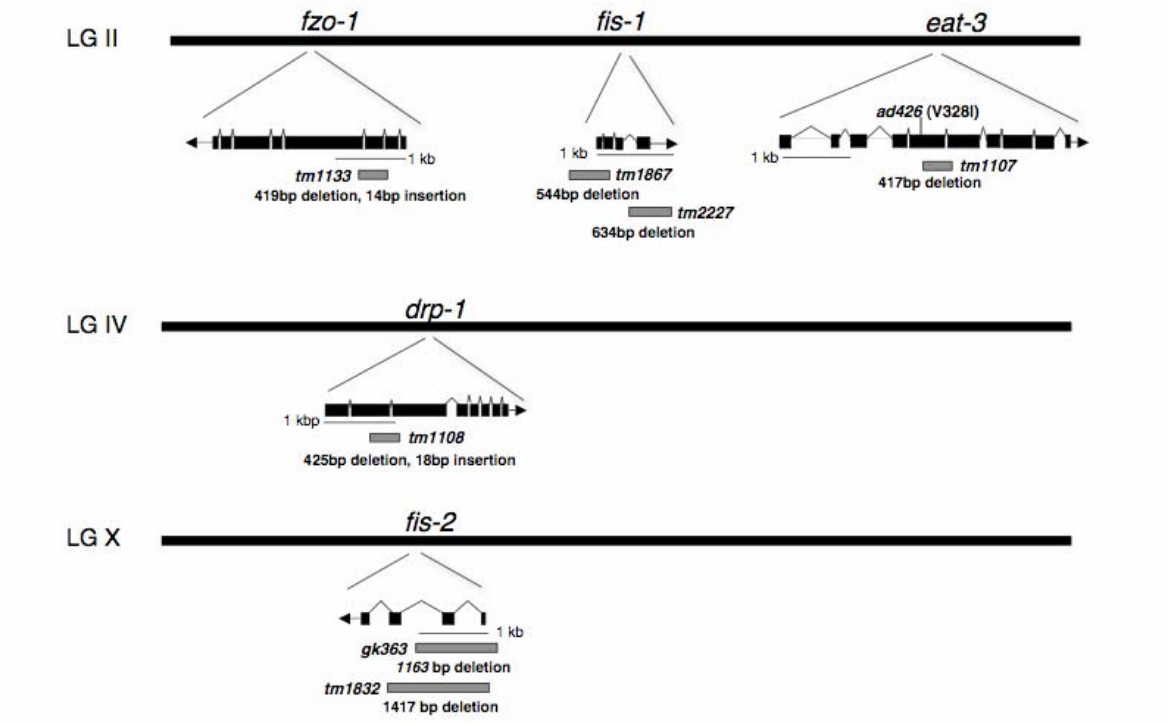

Figure S2. Schematic representations of deletions or mutations in the mitochondrial fission and fusion genes. LG, linkage group. Black boxes represent exons and waved lines indicate introns. Arrows pointed away from the boxes indicate the direction of transcription. Grey boxes represent the regions removed in each deletion allele. The actual size of each deletion (and in some cases with insertion) is indicated below the grey boxes.

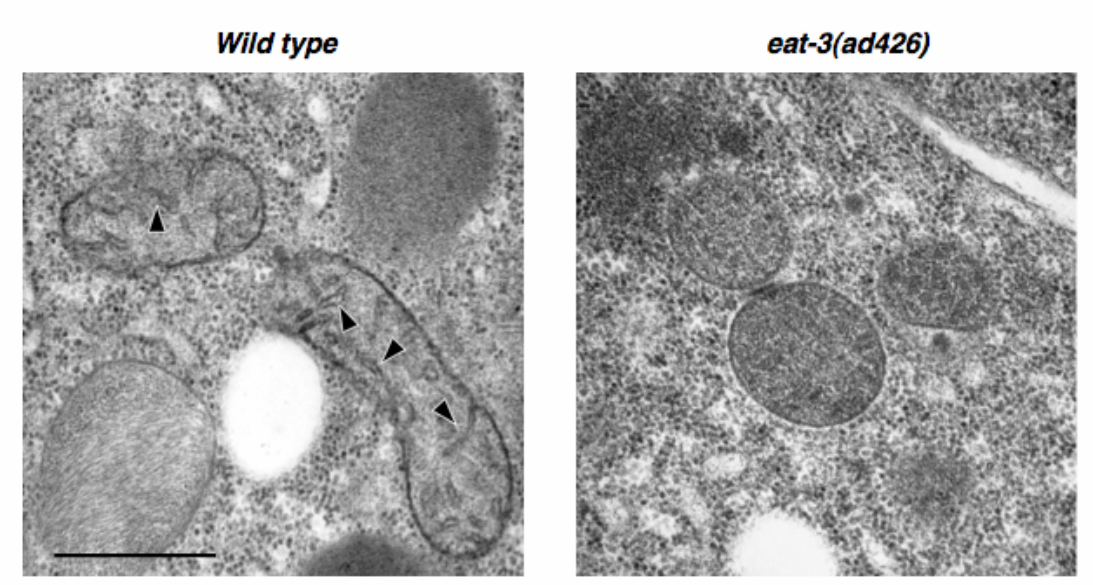

Figure S3. Disrupted cristae structure in the *eat-3(ad426)* mutant. Electron micrographs of the wild type (left) and the *eat-3(ad426)* (right) embryos. Arrowheads indicate normal cristae structure in mitochondria of the wild type embryo, which are absent or severely disrupted in mitochondria of the *eat-3(ad426)* embryo. Scale bar represents 0.5 μM.

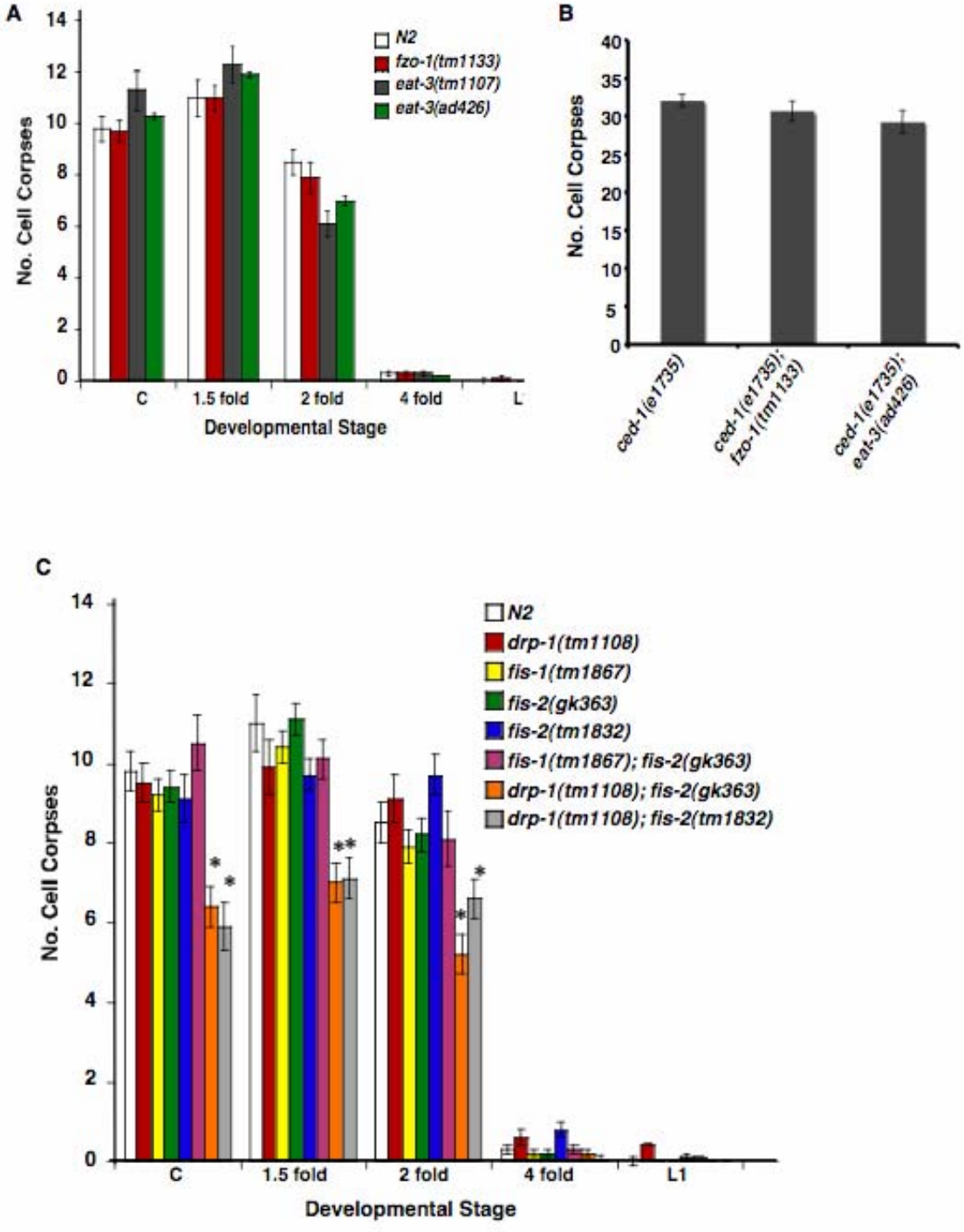
A
No. Cell Corpses
Developmental Stage
C
1.5 fold
2 fold
4 fold
L
N2
fzo-1(tm1133)
eat-3(tm1107)
eat-3(ad426)
B
No. Cell Corpses
ced-1(e1735)
ced-1(e1735); fzo-1(tm1133)
ced-1(e1735); eat-3(ad426)
C
No. Cell Corpses
Developmental Stage
C
1.5 fold
2 fold
4 fold
L1
N2
drp-1(tm1108)
fis-1(tm1867)
fis-2(gk363)
fis-2(tm1832)
fis-1(tm1867); fis-2(gk363)
drp-1(tm1108); fis-2(gk363)
drp-1(tm1108); fis-2(tm1832)

Figure S4. The kinetics of embryonic cell corpse appearance is not affected in the individual mitochondrial fission or fusion mutants. (A) Time-course analysis of cell corpse appearance during embryonic development in mitochondrial fusion mutants. Cell corpses were counted at the comma (C), 1.5-fold, 2-fold, and 4-fold embryonic stages, and the L1 larval stage. The Y-axis indicates the mean number of cell corpses scored in the head region of embryos or larvae. 15 animals were scored at each stage. (B) Analysis of the cell corpse numbers of mitochondrial fusion mutants in a sensitized *ced-1(e1735)* mutant background, which is defective in engulfment of cell corpses. Animals were scored as in (A) at the 4-fold stage embryos. (C) Time-course analysis of embryonic cell corpse appearance in *drp-1, fis-1* and *fis-2* mutants and corresponding double mutants. Cell corpses were counted as in (A). In all panels, error bars indicate the standard error of the mean. * Unpaired two tailed *t*-test, N2 vs. *drp-1(tm1108); fis-2(gk363)* at the comma, 1.5-fold and 2-fold stages: $P=2.8x10^{-5}$, $5.2x10^{-5}$, and $2.9x10^{-4}$, respectively; N2 vs. *drp-1(tm1108);fis-2(tm1832)* at the comma, 1.5 fold and 2 fold stages: $P=2.3x10^{-5}$, $9.8x10^{-5}$, and 0.043, respectively.

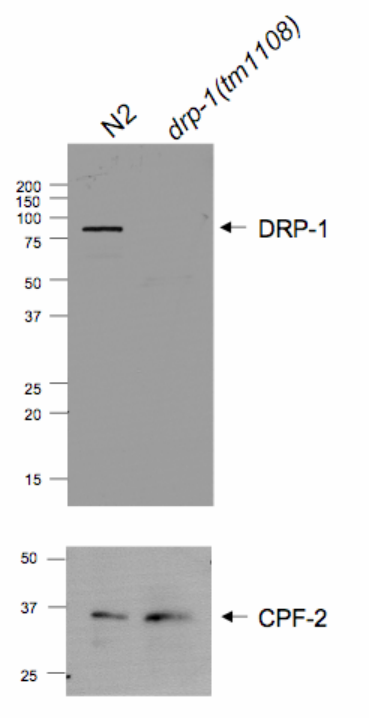

Figure S5. The *drp-1(tm1108)* deletion mutation results in a complete loss of the DRP-1 protein. Total worm lysates from *N2* and *drp-1(tm1108)* animals were resolved on a 10% SDS polyacrylamide gel, transferred to a nitrocellulose membrane, and then probed with anti-DRP-1 antibody (see Experimental Procedures). The CPF-2 protein was used as a loading control (Evans et al., 2001).

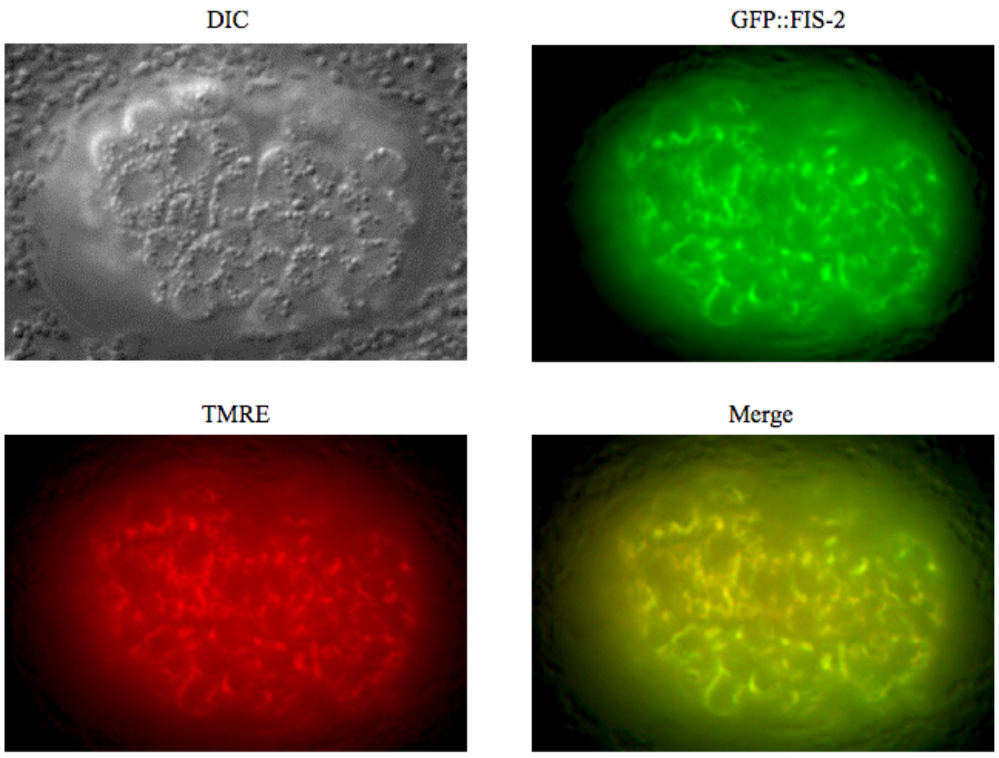

Figure S6. GFP::FIS-2 localizes to mitochondria in *C. elegans*. An embryo transgenic for the P_{hsp}*gfp::fis-2* constructs was stained with the mitochondria-specific dye TMRE, subjected to the heat-shock treatment to induce the expression of the GFP::FIS-2 fusion, and then visualized by fluorescent microscopy with Rhodamine and FITC filters. The merged image of GFP::FIS-2 and TMRE staining reveals extensive co-localization of GFP::FIS-2 with TMRE.

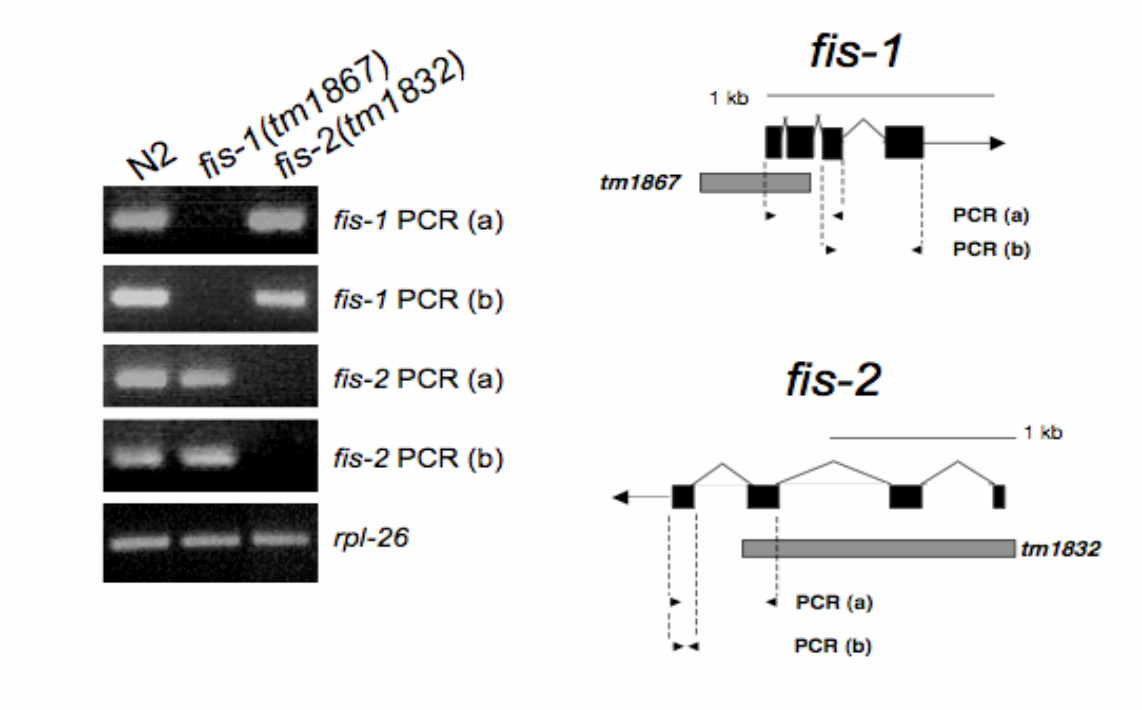

Figure S7. *fis-1(tm1867)* and *fis-2(tm1832)* deletion mutations result in complete loss of *fis-1* and *fis-2* expression, respectively. Reverse transcription was preformed on purified poly(A)$_n$ mRNA isolated from *N2, fis-1(tm1867),* and *fis-2(tm1832)* animals, followed by PCR amplification with primers specific to the coding regions of either *fis-1*, *fis-2*, or a control gene *rpl-26* (encoding a large ribosomal subunit L26 protein). The amplified PCR products in relation to the *fis-1* and *fis-2* genes are shown on the left. In each case, PCR (a) was conducted with one primer that is specific for a region within the respective gene deletion and one primer that lies outside of the deletion, whereas PCR (b) was conducted with primers lying outside of the gene deletions.

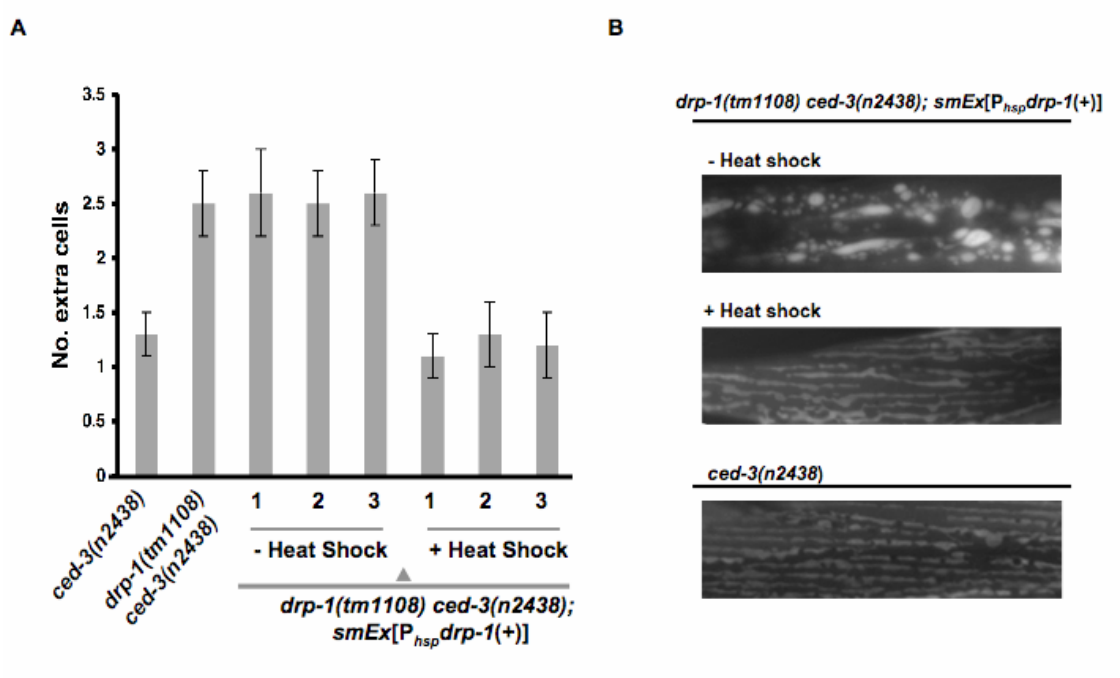

Figure S8. Overexpression of *drp-1* rescues the enhanced cell death defect in *drp-1(tm1108) ced-3(n2438)* animals. A) Three independent lines of *drp-1(tm1108) ced-3(n2438)* animals carrying a P_{hsp}*drp-1*(+) transgene were subjected to the heat-shock treatment (+ Heat Shock) at the embryonic stage as described in the Experimental Procedures or were not treated with heat-shock (- Heat Shock). The resulting larvae were analyzed for the number of extra cells in the anterior pharynx. Error bars indicate s.e.m. B). Overexpression of *drp-1* rescues the mitochondrial fission defect in *drp-1(tm1108) ced-3(n2438)* animals. Experiments were carried out as in (A), except that the embryos were allowed to develop into young adults and the muscle cell mitochondria labeled by P_{myo-3}*MitoGFP* were visualized by fluorescence microscopy.

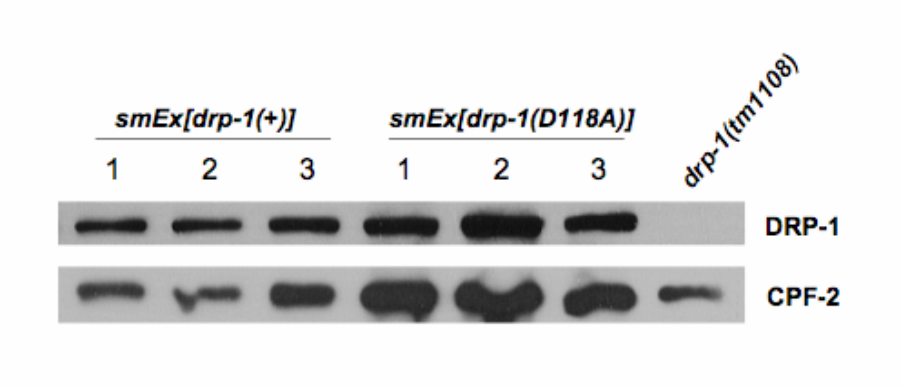

Figure S9. *drp-1*(+) and *drp-1*(D118A) transgenes express similar levels of the DRP-1 protein. Total worm lysates from three independent lines of *drp-1(tm1108) ced-3(n2438)* animals carrying either *smEx*[*drp-1*(+)] or *smEx*[*drp-1*(D118A)] transgenes were resolved on a 10% SDS polyacrylamide gel, transferred to a nitrocellulose membrane, and then probed with anti-DRP-1 antibody (see Experimental Procedures). The CPF-2 protein was used as a loading control (Evans et al., 2001).

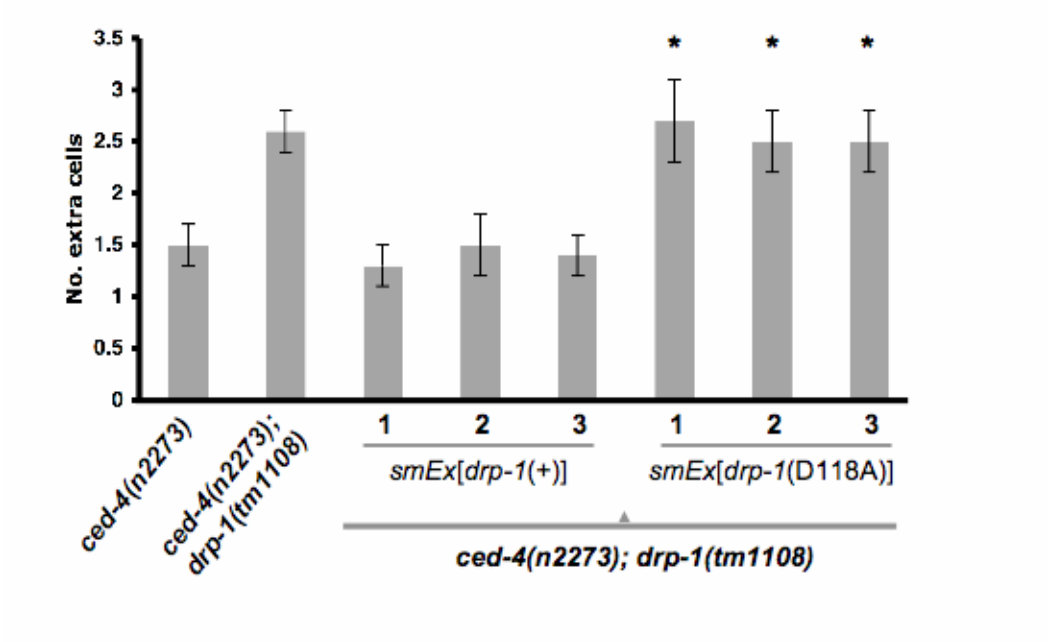

Figure S10. The enhanced cell death defect in *ced-4(n2273); drp-1(tm1108)* animals is rescued by *drp-1*(+) transgenes but not by *drp-1*(D118A) transgenes. *ced-4(n2273)*; *drp-1(tm1108)* animals carrying transgenes containing a 3994 bp *drp-1* genomic fragment [*drp-1*(+)] or the *drp*-1 genomic fragment harboring the DRP-1^{D118A} mutation [*drp-1*(D118A)] were analyzed for the number of extra cells in the anterior pharynx. Three independent transgenic lines were examined for each construct. Error bars indicate s.e.m. Unpaired two tailed *t*-test, compared with *ced-4(n2273)* animals: * $P < 0.005$.

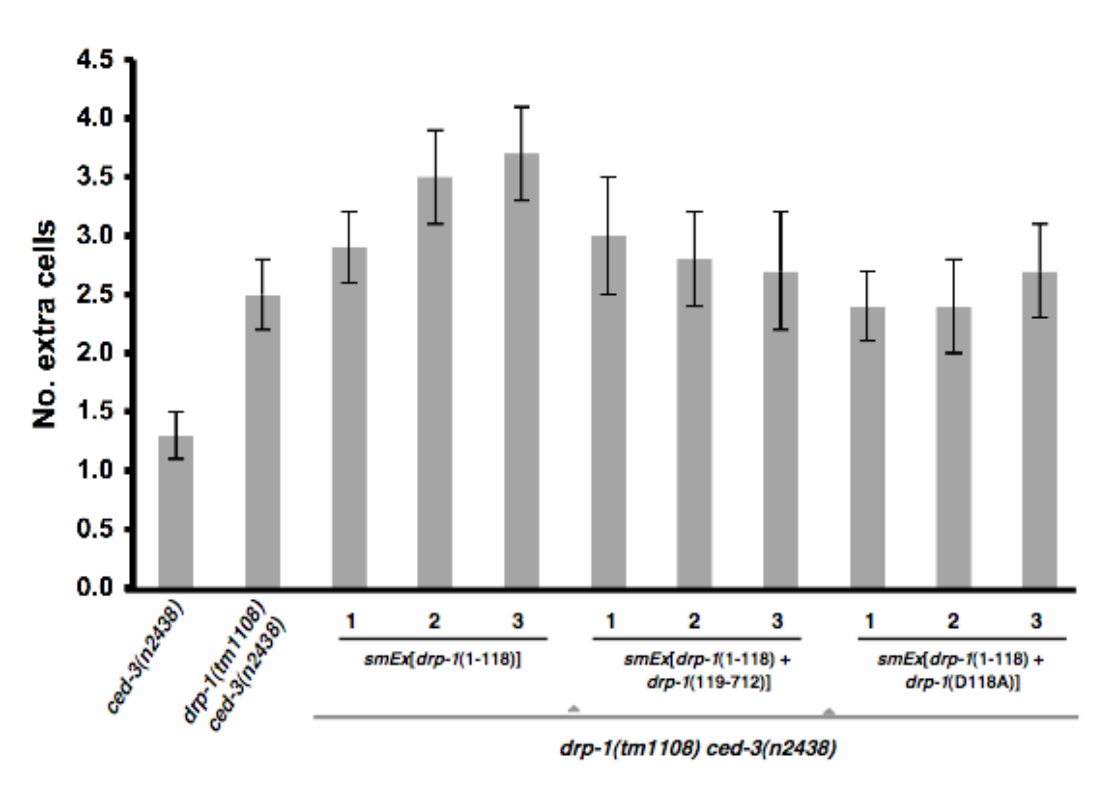

Figure S11. Expression of *drp-1*(1-118) or *drp-1*(119-712) alone or together does not rescue the enhanced cell death defect in *drp-1(tm1108) ced-3(n2438)* animals. *drp-1(tm1108) ced-3(n2438)* animals carrying the indicated transgene were analyzed for the number of extra cells in the anterior pharynx. Three independent transgenic lines were examined for each transgene. Error bars indicate s.e.m.

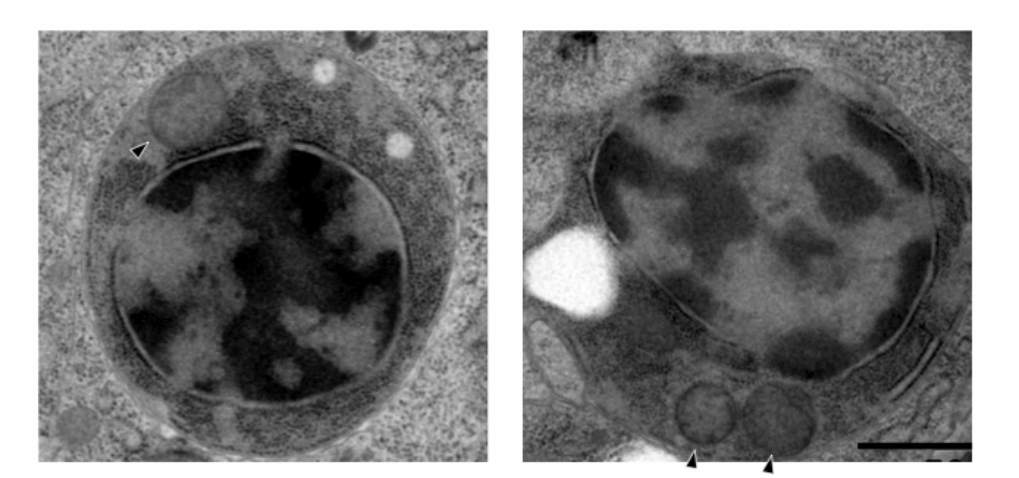

Figure S12. Mitochondria are fragmented in *ced-1(e1735); drp-1(tm1108)* corpses in the absence of DRP-1. The arrowhead marks a small and spherical mitochondrion similar to the ones seen in *ced-1(e1735)* cell corpses. Scale bar represents 0.5 μm.

Table S1. Overexpression of *drp-1*(K40A) inhibits apoptosis in *drp-1(tm1108)* animals to the same extent as in wild-type animals.

Genotype	Number of extra cells			
	Mean	s.e.m.	Range	n
N2	0.1	0.1	0-1	40
drp-1(tm1108)	0.1	0.1	0-1	30
+/+; *smEx*[P_{hsp}*drp-1*(K40A)] #1 - HS	0.1	0.1	0-1	20
+/+; *smEx*[P_{hsp}*drp-1*(K40A)] #2 - HS	0.1	0.1	0-1	20
+/+; *smEx*[P_{hsp}*drp-1*(K40A)] #3 - HS	0	0	0	20
+/+; *smEx*[P_{hsp}*drp-1*(K40A)] #4 - HS	0.1	0.1	0-1	20
+/+; *smEx*[P_{hsp}*drp-1*(K40A)] #1 + HS	1.2	0.2	0-3	20
+/+; *smEx*[P_{hsp}*drp-1*(K40A)] #2 + HS	1.0	0.1	0-3	20
+/+; *smEx*[P_{hsp}*drp-1*(K40A)] #3 + HS	0.8	0.2	0-3	20
+/+; *smEx*[P_{hsp}*drp-1*(K40A)] #4 + HS	1.0	0.2	0-3	20
drp-1(tm1108); smEx[P_{hsp}*drp-1*(K40A)] #1 - HS	0.1	0.1	0-1	20
drp-1(tm1108); smEx[P_{hsp}*drp-1*(K40A)] #2 - HS	0.1	0.1	0-1	20
drp-1(tm1108); smEx[P_{hsp}*drp-1*(K40A)] #3 - HS	0.2	0.1	0-1	20
drp-1(tm1108); smEx[P_{hsp}*drp-1*(K40A)] #4 - HS	0.1	0.1	0-1	20
drp-1(tm1108); smEx[P_{hsp}*drp-1*(K40A)] #1 + HS	0.8	0.2	0-2	20
drp-1(tm1108); smEx[P_{hsp}*drp-1*(K40A)] #2 + HS	1.1	0.2	0-3	20
drp-1(tm1108); smEx[P_{hsp}*drp-1*(K40A)] #3 + HS	1.0	0.2	0-3	20
drp-1(tm1108); smEx[P_{hsp}*drp-1*(K40A)] #4 + HS	0.9	0.2	0-2	20

Animals were injected with a construct that expresses *drp-1(K40A)* under the control of the heat-inducible promoter (P_{hsp}). Heat-shock treatment (+ HS) was carried out as described by Jagasia et al. (2005) and the number of extra cells in the anterior pharynx of the transgenic animals was scored as described in Experimental Procedures. For each experiment [with or without heat-shock treatment (- HS) or in wild-type (+/+) or *drp-1(tm1108)* background], four independent transgenic lines were scored (indicated by #). s.e.m., standard error of the mean. n indicates the number of transgenic animals scored.

Table S2. Overexpression of *fis-2* induces ectopic apoptosis independent of *drp-1*

Genotype	Number of cell corpses			
	Mean	s.e.m.	Range	n
N2	10.4	0.6	7-13	15
N2 (heat-shock control)	10.7	0.7	7-15	15
+/+; *smEx*[P_{hsp}*drp-1*] #1	8.4	0.5	5-13	15
+/+; *smEx*[P_{hsp}*drp-1*] #2	9.0	0.5	6-16	15
+/+; *smEx*[P_{hsp}*drp-1*] #3	9.6	0.8	6-18	15
+/+; *smEx*[P_{hsp}*fis-2*] #1	19.1	0.7	14-24	15
+/+; *smEx*[P_{hsp}*fis-2*] #2	14.1	1.2	8-23	15
+/+; *smEx*[P_{hsp}*fis-2*] #3	18.2	1.1	10-28	15
drp-1(tm1108); *smEx*[P_{hsp}*fis-2*] #1	18.3	0.9	11-25	15
drp-1(tm1108); *smEx*[P_{hsp}*fis-2*] #2	15.2	0.5	13-19	15
drp-1(tm1108); *smEx*[P_{hsp}*fis-2*] #3	17.2	0.8	12-23	15
+/+; *smEx*[P_{hsp}*fis-2*(1-124] #1	8.7	0.4	6-11	15
+/+; *smEx*[P_{hsp}*fis-2*(1-124] #2	8.6	0.4	6-11	15
+/+; *smEx*[P_{hsp}*fis-2*(1-124] #3	8.8	0.5	6-12	15

Animals were injected with the indicated construct that expresses *drp-1*, *fis-2*, or *fis-2(1-124)* under the control of the heat-inducible promoters. Protein expression was induced by heat-shock treatment at 33ºC for 40 minutes as described by Jagasia et al. (2005) and the number of cell corpses in the head region of 1.5-fold stage embryos was scored. For each experiment, three independent transgenic lines were scored (indicated by #). s.e.m., standard error of the mean. n indicates the number of transgenic embryos scored.

REFERENCES

C. elegans II (1997). Cold Spring Harbor Laboratory, Cold Spring Harbor.
Avery, L. (1993). The genetics of feeding in *Caenorhabditis elegans*. Genetics *133*, 897-917.
Brenner, S. (1974). The genetics of Caenorhabditis elegans. Genetics *77*, 71-94.
Evans, D., Perez, I., MacMorris, M., Leake, D., Wilusz, C. J., and Blumenthal, T. (2001). A complex containing CstF-64 and the SL2 snRNP connects mRNA 3' end formation and trans-splicing in *C. elegans* operons. Genes Dev. *15*, 2562-2571.
Jagasia, R., Grote, P., Westermann, B., and Conradt, B. (2005). DRP-1-mediated mitochondrial fragmentation during EGL-1-induced cell death in *C. elegans*. Nature *433*, 754-760.
Kamath, R. S., Martinez-Campos, M., Zipperlen, P., Fraser, A. G., and Ahringer, J. (2001). Effectiveness of specific RNA-mediated interference through ingested double-stranded RNA in *Caenorhabditis elegans.* Genome Biol. *2*, RESEARCH0002.
Labrousse, A. M., Zappaterra, M. D., Rube, D. A., and van der Bliek, A. M. (1999). *C. elegans* dynamin-related protein DRP-1 controls severing of the mitochondrial outer membrane. Mol. Cell *4*, 815-826.
Muller-Reichert, T., Hohenberg, H., O'Toole, E. T., and McDonald, K. (2003). Cryoimmobilization and three-dimensional visualization of *C. elegans* ultrastructure. J. Microsc. *212*, 71-80.
Wang, X., Yang, C., Chai, J., Shi, Y., and Xue, D. (2002). Mechanisms of AIF-mediated apoptotic DNA degradation in *Caenorhabditis elegans*. Science *298*, 1587-1592.